

## Final Technical Report

# QUANTIFYING UNCERTAINTIES IN PALEOLIQUEFACTION STUDIES

USGS NEHRP Award No. 06HQGR0013

PI: Scott M. Olson, PhD, PE  
University of Illinois at Urbana-Champaign  
2230d NCEL, MC-250  
205 N. Mathews Ave.  
Urbana, IL 61801  
Phone: 217.265.7584  
Fax: 265.8041 (fax)  
Email: [olsons@uiuc.edu](mailto:olsons@uiuc.edu)  
URL: <http://cee.uiuc.edu/Faculty/olson.htm>

co-PI: Y.K. Wen, PhD  
University of Illinois at Urbana-Champaign

Contributors: Junho Song, PhD  
Cora I. Johnson  
Kashif Muhammad

### NEHRP Element:

**Keywords:** Paleoliquefaction, liquefaction, seismic hazard, probability, Bayesian updating

*Research supported by the U.S. Geological Survey (USGS), Department of the Interior, under USGS Award No. 06HQGR0013. The views and conclusions contained in this document are those of the authors and should not be interpreted as necessarily representing the official policies, either expressed or implied, of the U.S. Government*

## **ABSTRACT**

Paleoliquefaction back-analysis using the magnitude bound and/or cyclic stress methods (or variants of these techniques) has become an important aspect of paleoseismic studies in regions where historical records are too short to assess earthquake recurrence and where active faults do not reach the ground surface. However, to date, paleoliquefaction studies have been solely deterministic and have not explicitly accounted for the numerous uncertainties involved in a paleoliquefaction back-analysis. In this study, we utilize simplified and rigorous statistical and probabilistic methods to quantify uncertainties in liquefaction susceptibility (aging and density change, liquefaction severity, fines content adjustment, and overburden stress correction); field data quality (field observations and in situ test measurements, ground failure mechanism, and field setting); and seismicity and seismic demand (attenuation relationships, magnitude scaling factor, depth reduction factor, and local site response). These uncertainties are combined in a Bayesian updating framework that uses the magnitude bound method to estimate a prior distribution, aggregate observations from individual paleoliquefaction site back-analyses to compute a likelihood function, and the product of the prior distribution and likelihood function to compute a posterior distribution for paleoearthquake magnitude. The proposed back-analysis procedure considering uncertainties yielded a preliminary  $M \sim 7.99 \pm 0.27$  for the Vincennes paleo-earthquake (circa 6100 years BP). This estimate is somewhat larger than deterministic estimates of 7.3 to 7.8 made by others, but provides explicit guidance on the reliability of the back-analysis and magnitude estimate.

## **NON-TECHNICAL SUMMARY**

The study of liquefaction features triggered by prehistoric, or paleo-, earthquakes is an important subset of a paleoseismology, particularly in regions like the central and eastern U.S. where the historical record is too short to adequately characterize earthquake recurrence intervals and faults do not extend to the ground surface where they can be directly studied. However, these “paleoliquefaction” back-analyses involve numerous uncertainties. In this study, we propose a combination of simplified and rigorous statistical and probabilistic methods to quantify many of these uncertainties. We then combine these uncertainties in a Bayesian updating framework that uses the magnitude bound method to provide a prior (or initial) distribution for earthquake magnitude, and updates this initial magnitude distribution using the aggregate observations from individual sites of paleoliquefaction features (i.e., the likelihood function for the occurrence of liquefaction). The product of the prior distribution and the likelihood function yields a posterior (or final) distribution for the magnitude of the paleoearthquake. This paleoearthquake magnitude considering uncertainties can be used in seismic hazard analyses to estimate the local, regional, and national hazard from potential future earthquakes. We applied the proposed procedure to a well-documented paleoearthquake in the Wabash Valley seismic zone of Indiana-Illinois (i.e., the Vincennes earthquake circa 6100 years BP) and preliminarily estimated a magnitude somewhat larger than other estimates for this event. However, the proposed procedure provides explicit guidance on the reliability of the back-analysis and magnitude estimate.

## **INTRODUCTION**

Quantifying uncertainties is an essential step in seismic hazard analysis, and it forms the basis for probabilistic seismic hazard analysis (PSHA) (e.g., Cornell 1968; Kulkarni et al. 1979; Algermissen et al. 1982; McGuire 2004). PSHA provides a framework to identify, quantify, and combine uncertainties from each aspect of seismic hazard, including: earthquake source(s) identification and characterization; recurrence relationships; and attenuation relationships. A logic tree approach (with subjective probability-weighted “input” parameters provides a convenient means to address epistemic (knowledge-based) uncertainty in a PSHA (e.g., Power et al. 1981; Kulkarni et al. 1984), while random variables can be used to address aleatory (intrinsic) uncertainty.

Probabilistic seismic hazard analysis has become increasingly useful because it is compatible with the current trend in practice and academia toward performance-based earthquake engineering (Somerville and Moriwaki 2003). However in regions that experience large, yet infrequent, earthquakes, the historical record often is too short to provide input for a PSHA, particularly regarding characteristic earthquake magnitudes and recurrence relationships. Furthermore, in regions where faults do not reach the ground surface, common paleoseismic methods such as surface rupture investigations or slip rate measurements generally cannot be used (McCalpin 1996). Therefore, investigators increasingly are studying secondary effects such as liquefaction to estimate ground motion characteristics for prehistoric earthquakes, even for events that occurred far back in Holocene time. This subset of paleoseismology is termed paleoliquefaction. Specifically, a paleoliquefaction study involves systematically searching for liquefaction features throughout a large geographic area, and then using those findings for quantitative back-analysis of the causative strength of shaking (Obermeier et al. 2005).

In this study, we outline many of the uncertainties that are involved in conducting a paleoliquefaction study. We use a combination of rigorous and approximate methods of uncertainty and reliability analysis to quantify many of the uncertainties that are routinely encountered in paleoliquefaction studies. The purpose of quantifying these uncertainties is for incorporation into seismic hazard analysis, particularly probabilistic seismic hazard analysis. Lastly, as a testbed case, we perform a quantitative uncertainty analysis for a paleoliquefaction study described by Green et al. (2005) of the Vincennes earthquake that occurred in the Wabash Valley seismic zone (WVSZ) circa 6100 years BP.

## **EXISTING APPROACHES FOR PALEOLIQUEFACTION STUDIES**

Two categories of analytical approaches are commonly used in paleoliquefaction studies to estimate seismic parameters. The first category involves using geotechnical procedures to determine earthquake ground motions required to induce liquefaction. The second category is referred to as the magnitude-bound method and entails the use of empirical correlations relating earthquake magnitude to the most distal sites of liquefaction. Recently, Olson et al. (2005a) introduced an integrated approach that combines tools from both of these categories. These approaches are briefly outlined below.

## Back-calculations using geotechnical procedures

Numerous liquefaction evaluation procedures have been proposed in literature, including stress-based (e.g., Seed and Idriss 1971), strain-based (e.g., Dobry et al. 1982), and energy-based methods (e.g., Green 2001). These approaches were developed for evaluating the liquefaction potential of soils at sites subjected to design (or future) earthquake motions. We refer to such use as “forward analysis.” However, in addition to forward analysis, liquefaction evaluation procedures have proven valuable for deterministically estimating the magnitude and associated peak ground acceleration at sites of liquefaction for pre-instrumental earthquakes (i.e., “back analysis”).

Of these methods, the most widely used is the stress-based procedure first proposed by Seed and Idriss (1971) and Whitman (1971). This empirical procedure was originally developed using observations of laboratory and field data, and has been continually refined by newer studies and by the increase in the number of liquefaction case histories (e.g., NRC, 1985; Seed et al., 1985; Youd and Idriss, 1997; Youd et al., 2001; Finn, 2002). The approach is based on using a semi-empirical estimate of the seismic demand and comparing this to an empirical estimate of liquefaction resistance estimated using in situ tests such as the standard penetration test (SPT), cone penetration test (CPT), or shear wave velocity (Vs). Olson et al. (2005a) describe this approach in detail. Here, we simply present the basic aspects of the approach to lead into our later discussion of uncertainties.

The seismic demand is a measure of the damage potential of the earthquake ground motions, and is normally characterized in terms of amplitude and duration. Seed and Idriss (1971) and Whitman (1971) proposed the following equation to estimate seismic demand:

$$CSR = \frac{\tau_{h,avg}}{\sigma'_{vo}} \approx 0.65 \frac{\tau_{h,max}}{\sigma'_{vo}} \approx 0.65 \frac{a_{max}}{g} \frac{\sigma_{vo}}{\sigma'_{vo}} r_d \quad [1]$$

where  $CSR$  = cyclic stress ratio;  $\tau_{h,avg}$  = average (equivalent) horizontal seismic shear stress  $\approx 0.65 \tau_{h,max}$ ;  $\sigma'_{vo}$  = initial vertical effective stress;  $a_{max}$  = peak ground acceleration (pga);  $g$  = acceleration of gravity;  $\sigma_{vo}$  = initial vertical total stress; and  $r_d$  = dimensionless stress reduction factor accounting for flexibility of the soil column.

Equation [1] constitutes the “simplified,” or approximate, procedure to estimate the amplitude of earthquake-induced *demand*. The  $r_d$  factor exhibits a wide range of values particularly at depths greater than 10 m, and the average value of the range is commonly used in engineering practice (Youd et al., 2001).

The duration of ground shaking is typically correlated to earthquake magnitude via magnitude scaling factors ( $MSF$ ).  $MSF$  are inversely proportional to the square root of duration of strong motion (Green and Mitchell, 2003) and are presented in reference to M 7.5 events. Figure 1 illustrates some of the numerous correlations for  $MSF$ . Youd and Idriss (1997) and Youd et al. (2001) describe the development of these relationships. As may be observed from this figure, the  $MSF$  vary greatly at all magnitudes, and particularly at magnitudes less than about 6.5.

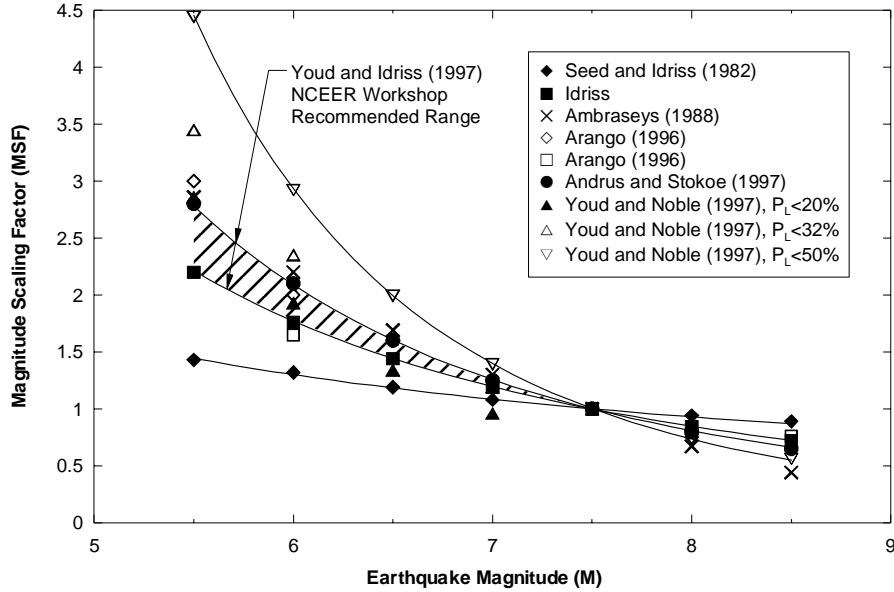


**Figure 1. Magnitude scaling factors proposed by various investigators (adapted from Youd and Noble, 1997).  $P_L$  is the probability of a liquefaction occurrence.**

In addition to  $MSF$ , the effect of overburden pressure on liquefaction resistance is incorporated in the cyclic stress method using the factor  $K_\sigma$ .  $K_\sigma$  adjusts the liquefaction resistance of a soil to the comparable value at one atmosphere effective confining stress. As discussed in Youd and Idriss (1997),  $K_\sigma$  is a function of the relative density of the soil, as well as the initial effective confining stress. Youd et al. (2001) provided relationships for  $K_\sigma$  at various values of relative density. The following expression constitutes the “simplified” approach to estimate seismic demand.

$$CSR_{M7.5} = 0.65 \frac{a_{\max}}{g} \frac{\sigma_{vo}}{\sigma'_{vo}} r_d \frac{1}{MSF} \frac{1}{K_\sigma} \quad [2]$$

Note that while  $K_\sigma$  actually applies to liquefaction resistance, it may be used to adjust the seismic demand, as above. Additionally, it should be noted that Eq. [2] applies *only* to free-field, level ground sites (i.e., slopes less than 6%).

The liquefaction resistance (or *capacity*) of the soil in the cyclic stress method is quantified in terms of cyclic resistance ratio ( $CRR$ ). Empirical correlations relating  $CRR$  to in-situ properties [e.g., SPT ( $N_1$ )<sub>60</sub>, CPT  $q_{T1}$ , or shear wave velocity  $V_{s1}$ ] were developed through the analysis of earthquake case histories. Sites containing sandy soils that were subjected to known (or reasonably estimated) earthquake motions were categorized as liquefied and non-liquefied, largely on basis of the presence or absence of surficial liquefaction features (e.g., sand boils). For each case history, the seismic demand was estimated using Eq. [3] and plotted as a function of the penetration resistance of the soil. The boundary giving a reasonable separation of the liquefied and non-liquefied points defines the  $CRR$  (or *capacity* curve). Figure 2 presents widely-used liquefaction resistance relationships that employ SPT-based case histories (Youd et al. 2001, as modified from Seed et al. 1985) and CPT-based case histories (Olson and Stark 1998).

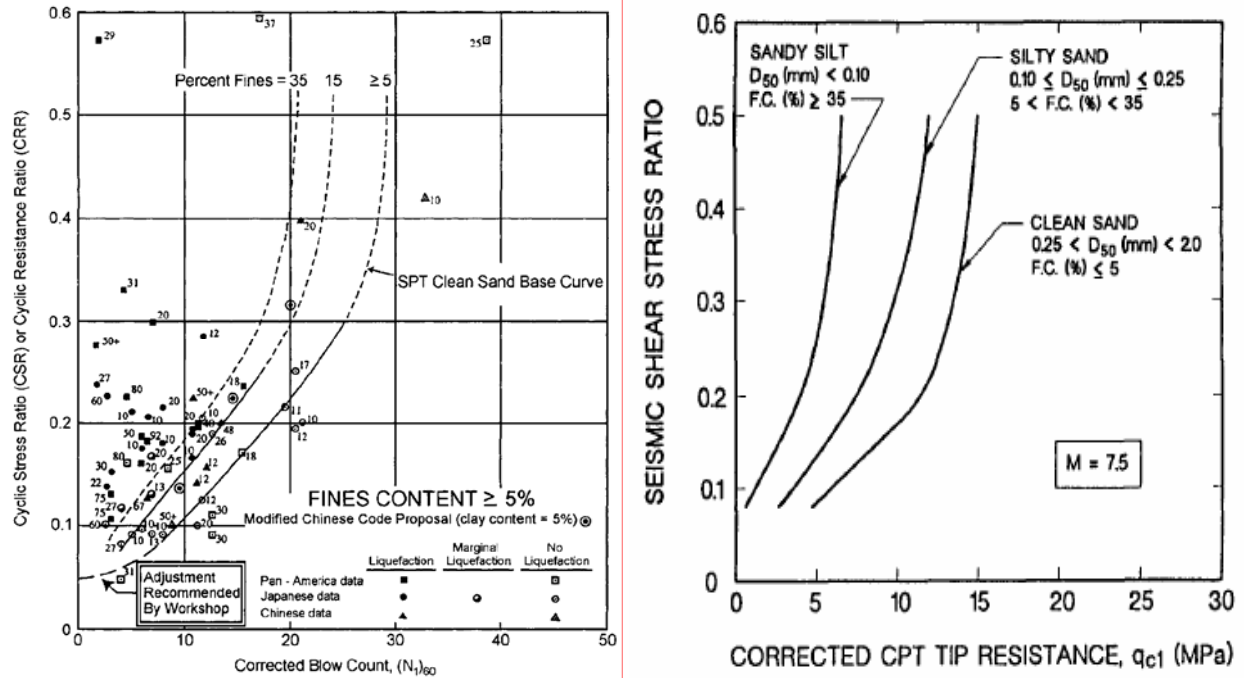


Figure 2. Liquefaction resistance curves for M 7.5 earthquakes. (a) Using liquefaction case histories where SPT are available (Youd et al. 2001, as modified from Seed et al. 1985); (b) using liquefaction case histories where CPT are available (Olson and Stark 1998).

The factor of safety against liquefaction ( $FS_{liq}$ ) is defined as the ratio of liquefaction resistance (or *capacity*) to seismic *demand*.

$$FS_{liq} = \frac{Capacity}{Demand} = \frac{CRR}{CSR_{M=7.5}} \quad [4]$$

Liquefaction is deterministically predicted when  $FS_{liq}$  is less than or equal to unity.

In a paleoliquefaction analysis, we are interested in estimating the strength of shaking required to trigger liquefaction. By rearranging Eq. (4) and substituting Eq (2) for  $CSR_{M=7.5}$ ,  $a_{max}$  can be expressed as a function of  $M$  and  $FS_{liq}$ :

$$a_{max} = \frac{CRR[(N_1)_{60cs}]}{FS_{liq}} MSF(M) K_{\sigma} \frac{g\sigma'_v}{0.65\sigma_v r_d} \quad [5]$$

### Magnitude bound method

Ambraseys (1988) collected data from around the world to define an empirical magnitude bound relation (i.e., a limiting, or maximum, distance to level-ground liquefaction features; see Figure 3), with the data primarily involving shallow crustal earthquakes along plate boundaries. This and similar relationships developed by others are widely employed in paleoseismic studies to estimate the magnitude of prehistoric earthquakes (e.g., Amick et al. 1990, Talwani and Schaeffer 2001, Street et al. 2004, among others).

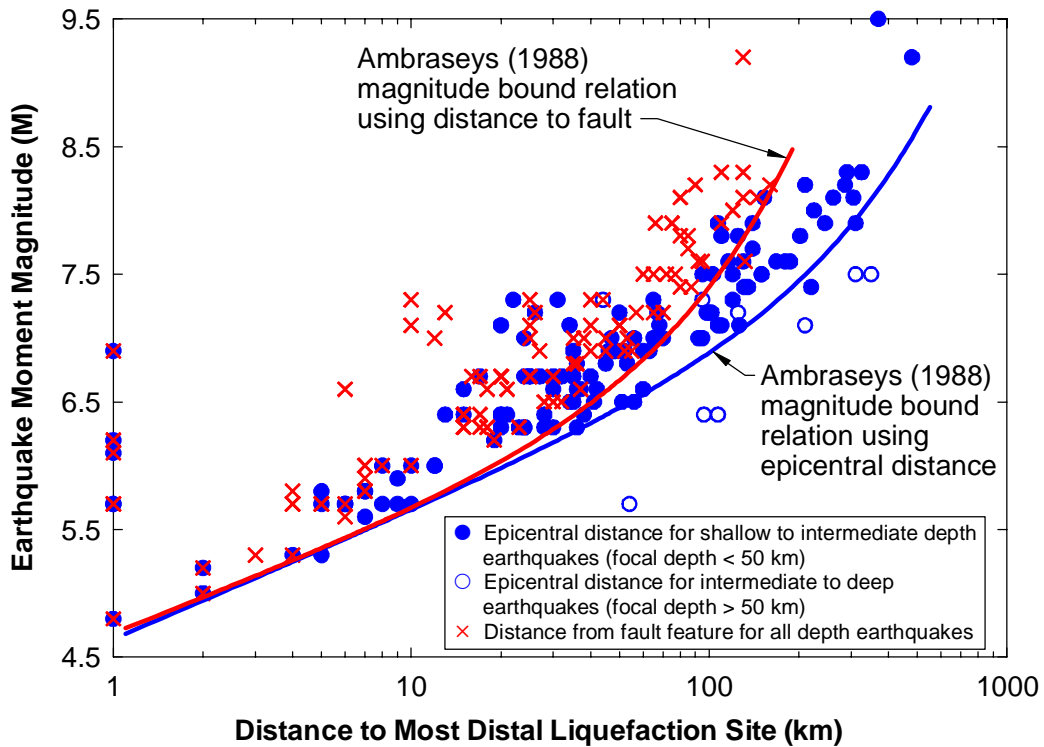


**Figure 3. Magnitude-bound relations for worldwide historical earthquakes using epicentral distance to most distal liquefaction site and distance from fault to most distal liquefaction site (from Ambraseys 1988)**

As discussed by Obermeier et al. (2001) and Olson et al. (2005a,b), paleomagnitude estimates using the magnitude bound method should be based on region-specific correlations rather than relations derived from worldwide data because the factors that control the maximum distance from the earthquake source at which liquefaction occurs are regionally dependent. These factors include: (1) earthquake source characteristics; (2) transmission characteristics (i.e., ground motion attenuation and local site effects); and (3) regional soil liquefaction susceptibility. For example, Obermeier et al. (1993) and Pond (1996) developed a region-specific magnitude bound relation for the Wabash Valley seismic zone (WVSZ), as presented in Figure 4. Pond and Martin (1997) and Obermeier and Pond (1999) then used this region-specific relation to interpret the magnitudes of a number of prehistoric earthquakes that occurred in the WVSZ during Holocene time (including the Vincennes earthquake that we will evaluate in a subsequent section of this report). More recently, Olson et al. (2005b) re-evaluated this bound for the based on updated estimates of the magnitude of historical earthquakes in the central and eastern U.S. (CEUS) and eastern Canada. Figure 4 includes their re-evaluated deterministic magnitude bound.

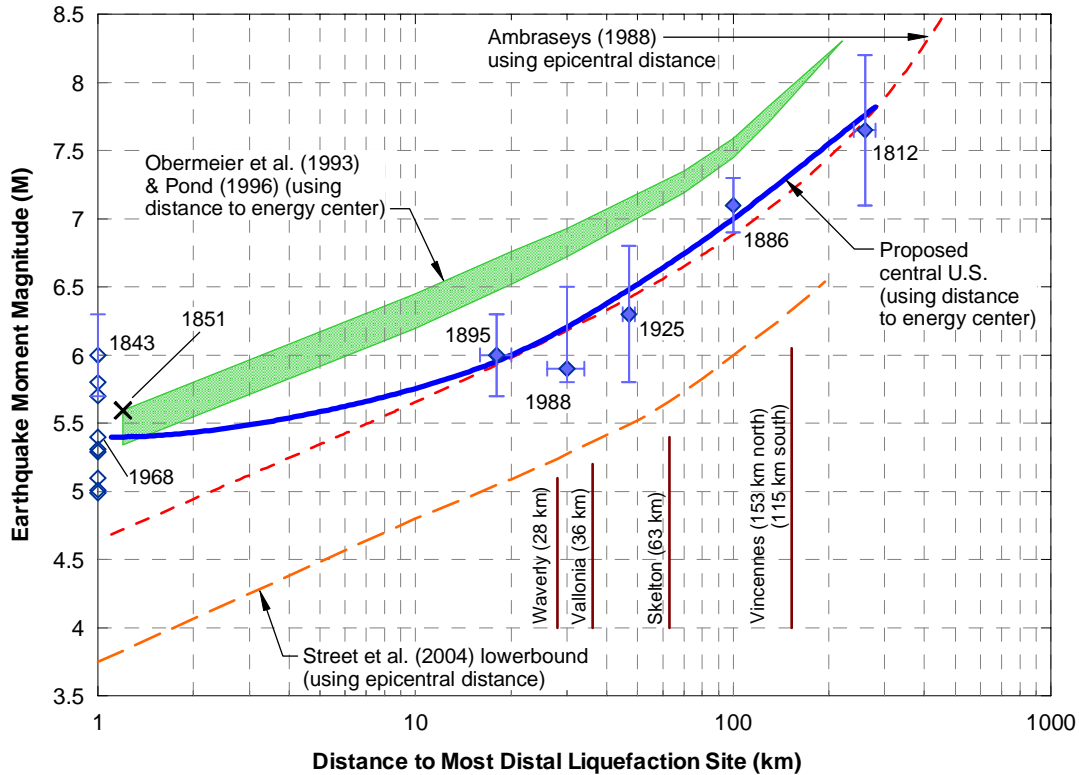


**Figure 4. Region-specific magnitude bound relation for central U.S. based on historical earthquakes in CEUS and eastern Canada compared with Ambraseys (1988) worldwide bound and region-specific relations developed by others for the Wabash Valley Seismic Zone. Solid symbols indicate reported liquefaction features associated with an earthquake. Open symbols indicate no reported liquefaction features associated with an earthquake. “X” symbol indicates liquefaction case reported by Pond (1996) in conjunction with 1851 “New Madrid” earthquake reported by Metzger (1996), which is not included in current historical CEUS earthquake databases (from Olson et al. 2005b).**

### Olson et al. (2005a) combined approach

Recently, Olson et al. (2005a) developed a new comprehensive approach that combines the cyclic stress method and the magnitude bound method. Figure 5 and the steps below summarize their approach.

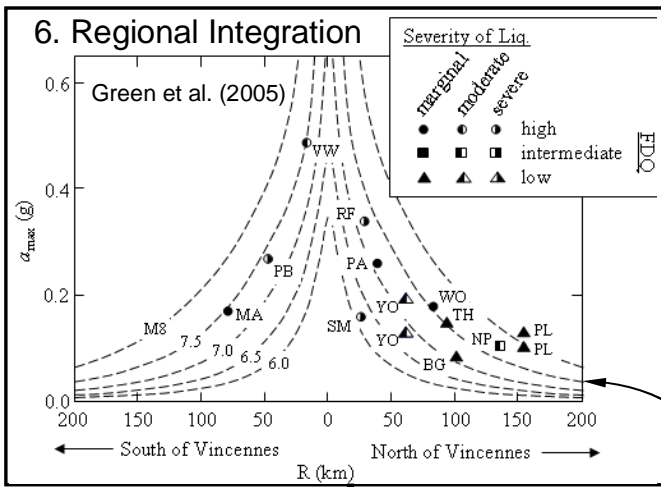
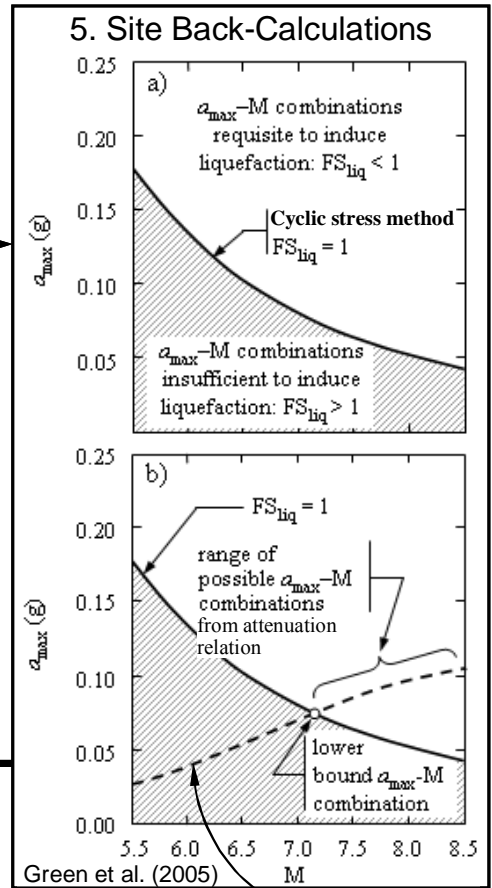
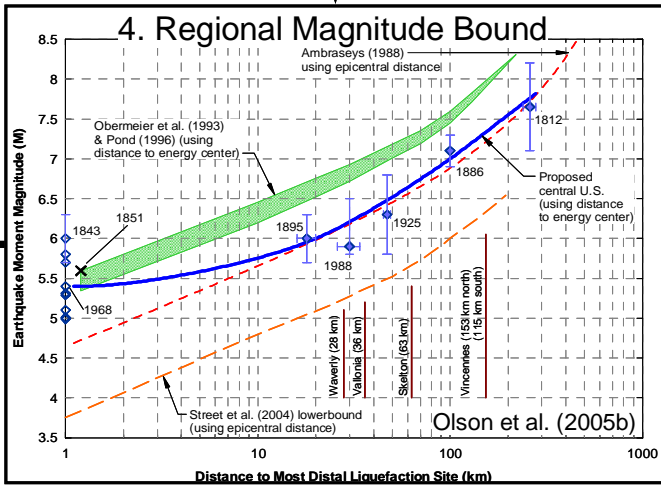
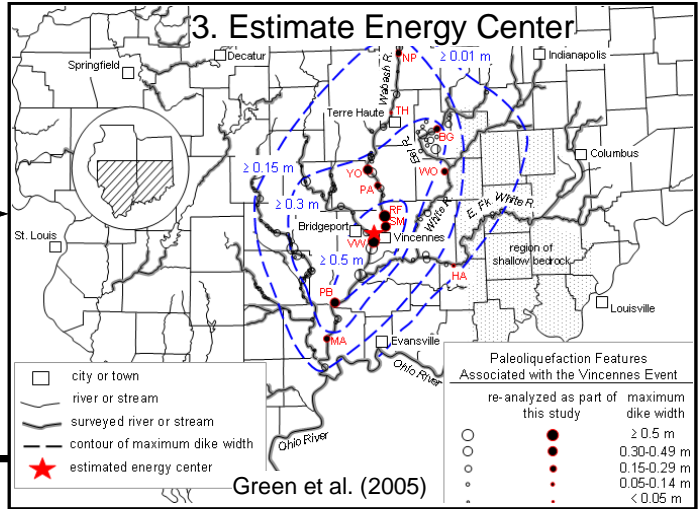
1. Plan field work with consideration of regional seismological and geotechnical issues that affect site selection, data interpretation, and details of back-analysis.
2. Perform field work using engineering geologic recommendations of Obermeier et al. (2001, 2005) and data collection techniques suggested by Olson et al. (2005a).
3. Estimate the provisional location of the paleoearthquake energy center.
4. Estimate paleomagnitude using a regional magnitude bound relationship and the distance from the energy center to the most distal site of liquefaction.
5. Perform back-calculations using liquefaction evaluation procedures at individual sites to estimate likely combinations of surface pga and  $M$  at each site.
6. Integrate results from individual sites into a regional assessment to verify the provisional energy center location and to estimate paleomagnitude.

### 1 & 2. Field Work

- Engineering geology
- Collect/interpret field data
- Assess potential aging effects



Obermeier (1998)



Estimates of M

### Site Response



Park & Hashash (2005)

Figure 5. Summary of Olson et al. (2005a) paleoliquefaction analysis procedure

## UNCERTAINTIES IN PALEOLIQUEFACTION STUDIES

As alluded to above, paleoliquefaction analyses involve numerous uncertainties (Olson et al. 2007). In the cyclic stress method, many of these uncertainties are related to: (1) liquefaction susceptibility (primarily aging, density change, and fines content); (2) field observations, ground failure mechanism, and field setting; (3) seismicity and seismic demand (i.e., attenuation relationships, magnitude scaling factors, and local site response; and (4) validity of in situ testing techniques, including selecting a representative penetration resistance. In the magnitude bound method, additional uncertainties occur due to the need to regionally calibrate the method using historic earthquakes in the same tectonic setting.

### Uncertainties related to liquefaction susceptibility

Liquefaction susceptibility refers to a sediment property/state (and other factors such as water table depth or artesian pressures) that affect a deposit's propensity to liquefy. The occurrence of liquefaction can drastically change the properties that influence subsequent liquefaction susceptibility. These changes relate mainly to changes in properties often associated with the passage of time (i.e., aging) and to changes in sediment density resulting from liquefaction (Olson et al. 2001). In addition, fines content and plasticity affect liquefaction resistance considerably.

Aging is defined as the process by which natural and man-made deposits develop a structure over time that results in improved soil properties such as increased shear strength, stiffness, and penetration resistance (Schmertmann 1991). Aging effects are attributed to mechanical sources (e.g., secondary compression and preshearing) and chemical sources (i.e., cementation and bonding). The net result of aging is an increased resistance to liquefaction (i.e., reduced liquefaction susceptibility). However, the actual changes in liquefaction susceptibility that occur over time can be either large or very small and can vary greatly from geographic region to region.

The occurrence of liquefaction results in an increase in density as shaking-induced porewater pressures dissipate and the soil reconsolidates. But this density increase may or may not result in an increase in liquefaction resistance. The reason for a potential decrease in liquefaction resistance following liquefaction is the destruction of the pre-earthquake (aged) soil structure (Terzaghi et al. 1996; Oda et al. 2001; Olson et al. 2001).

For paleoseismic analysis, the implication of these factors is as follows. Data collected for the cyclic stress method were obtained shortly after the causative earthquakes. When collected, these data had experienced some density change, but potentially little post-earthquake aging. However, in situ data collected for a paleoliquefaction study are necessarily obtained hundreds or thousands of years after the causative earthquake. In order for the cyclic stress method to be applied appropriately, recently-collected in situ data potentially need to be "corrected" for aging to the deposit's condition shortly after the causative earthquake. This can lead to significant uncertainty in estimating the strength of shaking required to trigger liquefaction. For example, Olson et al. (2001) describe an example where this "correction" led to a factor of 2 difference in  $p_{ga}$ .

Green et al. (2006) detail the effects of low plasticity fines on liquefaction resistance measured in the laboratory and observed from field case histories. They argue that in contrast to widely used liquefaction resistance relationships, sands with high fines contents (i.e., greater than 30 – 40%) may be more susceptible to liquefaction than previously thought. Both this potential effect and the role of fines plasticity are areas of active research and constitute uncertainties for paleoliquefaction analyses.

### **Uncertainties related to field observations, ground failure mechanism, and field setting**

Factors such as the water table and source bed depth, the presence and thickness of a fine-grained cap, and the presence of a free-face or sloping ground at the time of the causative earthquake all must be inferred from geologic field observations. Thus, these factors add uncertainty to paleoliquefaction back-analyses at individual sites.

In addition, the data in Figure 2 and Figure 3 exclusively involve field observations made in plan view. For these data, investigators designated sites as “liquefied” based on the presence of surficial liquefaction evidence, such as sand blows, ground cracking, surface settlements, etc. However, most paleoliquefaction studies are performed in sectional view, e.g., by observing stream banks. Therefore, there is some uncertainty regarding whether features observed in sectional view would be observed in plan view, and regarding the severity of liquefaction observed in sectional and plan view.

The data in Figure 2 and Figure 3 also incorporate all mechanisms of ground failure – hydraulic fracturing, lateral spreading, and surface oscillations. But the ground failure mechanism may control whether surface manifestations of liquefaction develop for some field settings and from some intensities of earthquake shaking (Obermeier et al. 2001). For example, liquefaction features may not manifest at the surface of a level site when an overlying fine-grained cap is relatively thick or when the water table is located below the top of the liquefied stratum. Accordingly, it seems likely that some of the “no liquefaction” data in Figure 2a are sites that actually did liquefy – and may be identified as such in a paleoliquefaction study conducted in sectional view. Similarly, liquefaction likely occurs beyond the farthest site-to-source distance that is used for the magnitude bound method (Figure 3), but such occurrences cannot be discerned in plan view. Together, these factors lead to uncertainty in using limiting relations like those in Figure 2 and Figure 3 for paleoliquefaction back-analysis.

### **Uncertainties related to seismicity and seismic demand**

Several factors related to seismicity lead to uncertainty in using the cyclic stress method for paleoliquefaction analysis. The first two factors relate to the liquefaction resistance curve shown in Figure 2. In some cases, the site data do not have very well constrained values of  $p_{ga}$ , even for recent earthquakes. Furthermore, it is widely known that the shaking intensity can vary greatly in a short distance horizontally. These two factors can lead to substantial errors in the estimated seismic demand for individual data and potential uncertainties in paleoliquefaction analysis. In addition to the uncertainty associated with estimating the seismic demand amplitude, the duration of seismic demand, as represented by an “equivalent number of cycles” (i.e., a magnitude scaling factor, or MSF, in the cyclic stress method) also may be highly uncertain. For

example, various MSFs range from roughly 1.2 to 2.0 for  $M = 6.5$ , although the “recommended” range varies from only about 1.4 to 1.6.

There also is considerable uncertainty in applying various regional attenuation relations, the effects of local site response, and selecting representative acceleration time histories if site response analyses are performed. For example, predicted median values of  $pga$  for *rock* sites (excluding site effects) in the central U.S. vary by about a factor of 2 at most site-to-source distances. Site response effects (especially for soft soil sites, including liquefiable deposits) can exacerbate this uncertainty and exhibit ground motion amplification factors that vary from about 1 to 6 and about 0.6 to 3 for weak and moderate ground motions, respectively (Idriss 1990).

Lastly, in some cases it is not clear whether multiple, widespread paleoliquefaction occurrences were triggered by a single large earthquake or several smaller earthquakes occurring in the same region at about the same time. Generally, if multiple smaller earthquakes did occur, it is not possible to discern differences in the ages of features caused by these earthquakes using radiocarbon, geological, or archeological dating techniques. Green et al. (2005) discuss a deterministic approach to evaluate this question, but clearly this issue adds uncertainty to an estimate of paleomagnitude.

### **Uncertainties related to in situ testing techniques**

Uncertainties related to in situ testing include: (1) finding measurable differences in test results between sites that did and did not liquefy; (2) the repeatability and interpretation of various in situ tests (e.g., standard penetration test, cone penetration test, shear wave velocity measured by various methods); (3) the ability to measure the properties of thin liquefiable layers using various in situ tests; and (4) selecting a “representative” in situ test value from multiple tests (Olson et al. 2005a). The last item potentially leads to the largest uncertainty, and is highlighted below. These uncertainties are affected by the testing device and procedures, the spatial distribution of soil types and soil properties, and subjective interpretation of the test results.

### **Uncertainties in magnitude bound method**

The magnitude bound method has other unique uncertainties in addition to those mentioned previously, including: (1) estimates of  $M$  for individual data, particularly for pre-instrumental earthquakes; (2) the role of regional conditions on the position of the boundary curve (Olson et al. 2005a,b); and (3) estimates of “energy centers” for paleoearthquakes. Ambraseys (1988) suggested that potential errors in  $M$  are about  $\pm 0.25$  to 0.5 for recorded events, and at least that great for pre-instrumental events. The location of a limiting boundary is necessarily region-specific and a function of the most optimal combination of: earthquake source characteristics; transmission characteristics (i.e., ground motion attenuation and local site effects); and regional soil liquefaction susceptibility. As a result, magnitude bound relations for specific regions may (or may not) vary considerably from the bound for worldwide data, which necessary extends to the softest sites with the most favorable transmission and site response effects. Lastly, because energy centers for paleoearthquakes often are estimated from the distribution and sizes of liquefaction features, these energy centers may differ in location from either an instrumental

epicenter or a distance to fault (site-to-source distance) commonly used in magnitude bound relations.

## **FRAMEWORK FOR TREATING UNCERTAINTIES**

### **Treating liquefaction susceptibility**

As mentioned previously, post-liquefaction aging may constitute a significant uncertainty when conducted paleoliquefaction studies in some geologic settings. To evaluate the significance of post-liquefaction aging in a general sense, we collected a large database of liquefaction and no liquefaction case records where CPT results were available. Table 1 presents the liquefaction/no liquefaction database. Following the thought of Newman (2007), Table 1 includes the time elapsed following an earthquake until in situ testing was performed.

Using the times shown in Table 1, an average of approximately 1030 days (2.8 years) elapsed after the causative earthquake before in situ penetration resistance data (i.e., SPT or CPT such as those shown in Figure 2) was collected. The minimum time that elapsed was 45 days and the maximum elapsed time was 7050 days (19.3 years). As a result, considerable time for aging had passed prior to measuring penetration resistance. Table 2 summarizes several potential combinations. As illustrated in the table, it is quite likely that 2 to 3 log cycles of aging has occurred.

Olson et al. (2005a) argued that a significant portion of the mechanical aging that occurs in situ takes place in the first few log cycles of time following post-liquefaction reconsolidation, which is consistent with the penetration resistance increases discussed by Mesri et al. (1990). If this hypothesis is correct, that means that aging effects (during Holocene time) may be of secondary importance to paleoliquefaction studies. This is consistent with the observations that the minimum SPT blow counts measured in freshly deposited point bar sands is 0 to 1 blows/0.3 m (S. Obermeier, 2006, personal communication), while the minimum SPT blow counts measured in the loosest deposits that liquefied during the Vincennes earthquakes are about 3 blows/0.3 m. Therefore, even in the loosest sands, the mechanical aging effects are not likely to amount to more than 2 or 3 blows/0.3 m in this region over approximately 5000 calendar years (i.e., approximately 5 to 6 log cycles of time). Furthermore, we anticipate that Holocene sands that are denser (i.e., have higher SPT blow counts) are likely to experience even smaller aging increases.

**Table 1. Database of liquefaction/no liquefaction case records where CPT results are available**

Case No.	Eq. M	Earthquake	Site	CPT No.	days after eq.	Liq. Severity	Failure Mech.	Reference	depth (m)	gwt depth (m)	$\gamma_{tot}$ (kN/m <sup>3</sup> )	F.C. %	$\sigma'_v$ (kPa)	$q_c$ (MPa)	$q_{c1}$ (MPa)	$(q_{c1})_{cs}$ (MPa)	$a_{max}$ (g)	CSR (MPa)	FS <sub>liq</sub>
1	5.3	1957 Daly City, CA	Marina District	M1	n/a	0	--	Bennett (1990);	3.0	2.3	19	2	50.1	5.5	7.5	7.5	0.20	0.05	2.40
2			Marina District	M2	n/a	0	--	Gilstrap & Youd (1998);	3.0	2.7	19	3	54.1	6.3	8.4	8.4	0.20	0.05	2.87
3			Marina District	M3	n/a	0	--	Toprak et al. (1999)	3.0	2.7	19	3	54.1	7.1	9.6	9.6	0.20	0.05	3.24
4			Marina District	M4	n/a	0	--		4.2	2.9	19	5	67.0	2.6	3.1	3.1	0.20	0.05	1.08
5			Marina District	M6	n/a	0	--		6.2	5.5	19	4	110.9	4.0	3.8	3.8	0.20	0.05	1.44
6	7.5	1964 Niigata, Japan	Kawagishi-Cho building		7050	3	HF	Ishihara and Koga (1981);	3.7	1.1	18	5	41.3	1.6	2.4	2.4	0.16	0.16	0.29
7			South bank		7050	0	--	Farrar (1990)	1.5	0.5	18	5	17.2	6.5	11.1	11.1	0.16	0.16	1.12
8	6.4	1971 San Fernando	Juvenile Hall	2-B1	3860	3	LS	Youd (1973);	9.0	8.3	18	50	155.1	3.3	2.5	9.0	0.50	0.20	0.74
9			Juvenile Hall	4-B2	3860	3	LS	Bennett (1989);	6.7	6.1	18	67	114.7	2.5	2.3	8.2	0.50	0.20	0.66
10			Juvenile Hall	6-B1	3860	3	LS	Bennett et al. (1998);	4.7	4.3	18	74	80.7	1.1	1.2	4.4	0.50	0.21	0.37
11			Juvenile Hall	10-B1	3860	3	LS	Toprak et al. (1999)	5.5	4.7	18	65	91.2	1.8	1.9	6.7	0.50	0.21	0.53
12			Juvenile Hall	11-B1	3860	3	LS		6.8	5.7	18	61	111.6	2.7	2.5	9.0	0.50	0.21	0.69
13			Balboa Blvd	Bal-10	n/a	0	--		8.3	7.2	18.5	36	142.8	3.5	2.8	10.1	0.45	0.18	0.89
14			Wynne Ave.	Wyn-1	n/a	0	--		7.8	4.7	18.5	16	113.9	4.9	4.6	7.9	0.25	0.12	1.07
15			Wynne Ave.	Wyn-5a	n/a	0	--		7.6	4.3	18.5	31	108.2	4.1	3.9	12.4	0.25	0.12	1.73
16	7.3	1975 Haicheng, China	Chemical Fiber Bldg		3650	1	HF	Arulanandan et al (1986)	5.0	1.5	18	61	55.7	0.8	1.1	3.8	0.15	0.14	0.48
17			Construction Bldg		3650	2	HF		6.5	1.5	18	83	68.0	0.6	0.7	2.4	0.15	0.15	0.32
18			Fishery and Shipbuilding		3650	2	HF		3.0	0.5	18	90	29.5	0.9	1.5	5.2	0.15	0.16	0.56
19			Glass Fiber Bldg		3650	2	HF		5.0	0.8	18	42	48.3	1.8	2.5	9.0	0.15	0.16	0.90
20			Paper Mill		3650	2	HF		4.0	1.0	18	72	42.6	0.7	1.0	3.6	0.15	0.15	0.45
21			Middle School		3650	0	--		9.5	1.0	18	73	87.6	0.8	0.9	3.0	0.15	0.16	0.35
22	5.6	1977 Matata, New Zealand	Robinson Farm east	cpt1	2500	1	LS	Christensen (1995)	3.6	0.8	13.5	7	20.7	3.5	6.0	6.0	0.25	0.16	0.65
23			Robinson Farm west	cpt4	2500	1	LS		1.8	0.6	13.5	7	12.6	3.7	6.3	6.3	0.25	0.13	0.82
24			Morris Farm	cpt1	2500	0	--		3.5	1.6	13.5	9	28.7	7.5	12.4	13.3	0.15	0.07	4.06
25	6.6	1979 Imperial Valley, CA	Heber Road	S4	75	3	LS	Youd & Bennett (1983);	2.2	1.8	18	23	35.7	1.4	2.2	5.4	0.60	0.29	0.32
26			Heber Road	S1	75	0	--	Bennett et al. (1981);	4.0	1.8	19	10	54.4	13.2	17.7	20.7	0.60	0.36	14.38
27			Heber Road	S7	75	1	LS	Baziar et al. (1992);	2.3	1.8	19	28	38.8	3.0	4.5	13.1	0.60	0.30	0.84
28			Kornbloom Road	K4	n/a	0	--	Moss (2003);	3.0	2.5	18	62	49.1	1.7	2.4	8.6	0.08	0.04	3.64
29			Radio Tower	R2	n/a	2	HF	Bennett et al. (1984);	3.3	2.0	18	64	46.6	1.1	1.6	5.7	0.22	0.12	0.81
30			Radio Tower	R4	n/a	0	--	Youd & Wiecezorek (1982);	2.3	2.0	18	18	38.5	5.8	8.8	16.9	0.22	0.10	10.05
31			River Park	RP4	75	3	HF	Gilstrap & Youd (1998)	1.1	0.1	18	88	9.5	1.5	2.5	8.9	0.20	0.18	0.78
32			Vail Canal	V2	n/a	0	--		5.1	3.0	18	12	71.2	5.6	6.6	9.0	0.13	0.07	2.04
33			McKim Ranch	M7	n/a	2	HF		2.8	1.5	18	20	37.6	3.0	4.6	9.7	0.44	0.26	0.61
34			Wildlife site	3Cg	n/a	0	--		3.0	1.9	18	60	43.2	1.5	2.2	7.8	0.17	0.09	1.38
35	6.0	1981 Westmorland, CA	Kornbloom Road	K4	500	2	HF	Bennett et al. (1984);	3.0	2.5	18	62	49.1	1.7	2.4	8.6	0.28	0.10	1.38
36			Radio Tower	R2	500	1	HF	Youd & Wiecezorek (1982);	3.3	2.0	19	64	49.9	1.1	1.6	5.6	0.18	0.07	1.30
37			Radio Tower	R4	500	0	--	Baziar et al. (1992)	2.3	2.0	20	18	43.1	5.8	8.4	16.3	0.18	0.06	12.33
38			Vail Canal	V2	500	2	LS		5.1	3.0	18	12	71.2	5.6	6.6	9.0	0.26	0.11	1.35
39			McKim Ranch	M7	500	0	--		2.8	1.5	19	20	40.4	3.0	4.5	9.4	0.12	0.05	2.95
40			Wildlife site	3Cg	500	2	LS		3.0	1.9	18	60	43.2	1.5	2.2	7.8	0.23	0.09	1.35
41	6.0	1987 Elmore Ranch, CA	Wildlife site	3Cg	500	0	--	Baziar et al. (1992)	3.0	1.9	18	60	43.2	1.5	2.2	7.8	0.13	0.05	2.39
42	6.6	1987 Superstition Hills, CA	Wildlife site	3Cg	500	2	LS	Holzer et al. (1989)	3.0	1.9	18	60	43.2	1.5	2.2	7.8	0.21	0.11	1.12
43	5.9	1988 Sanguenay, Quebec, Canada	Site 1; sand boil A	Site 1	n/a	1	HF	Tuttle et al. (1990b)	4.5	1.7	18	15	53.5	2.8	3.8	6.2	0.25	0.12	0.90
44	6.6	1987 Edgecumbe, New Zealand	Landing Bridge Road	cpt10	2500	3	LS	Christensen (1995);	4.0	1.5	15	5	35.3	3.5	5.5	5.5	0.27	0.20	0.47
45			James Street Loop	cpt4	2500	3	LS	Moss (2003)	4.4	2.0	15	5	42.5	3.9	5.7	5.7	0.28	0.19	0.52
46			Whatakane Pony Club	cpt2	2500	2	LS		5.3	2.4	15	16	50.6	4.2	5.8	10.2	0.28	0.19	0.88
47			Robinson Farm east	cpt1	2500	3	Indet.		3.6	0.8	13.5	7	20.7	3.5	6.0	6.0	0.44	0.45	0.23
48			Robinson Farm west	cpt4	2500	2	LS		1.8	0.6	13.5	7	12.6	3.7	6.3	6.3	0.44	0.37	0.28
49			Gordon Farm	cpt1	2500	2	HF		3.5	0.5	13.5	0	17.5	2.7	4.6	4.6	0.43	0.50	0.16
50			Gordon Farm	cpt2	2500	0	--		1.8	0.9	13.5	0	15.5	7.4	12.5	12.5	0.43	0.30	0.74
51			Brady Farm	cpt1	2500	2	HF		3.0	1.7	13.5	56	27.3	1.7	2.9	10.1	0.40	0.26	0.63

Case No.	Eq. M	Earthquake	Site	CPT No.	days after eq.	Liq. Severity	Failure Mech.	Reference	depth (m)	gwt depth (m)	$\gamma_{tot}$ ( $kN/m^3$ )	F.C. %	$\sigma'_v$ (kPa)	$q_c$ (MPa)	$q_{c1}$ (MPa)	$(q_{c1})_{cs}$ (MPa)	$a_{max}$ (g)	CSR (MPa)	$FS_{liq}$
52			Brady Farm	cpt4	2500	0	--		3.8	1.5	13.5	15	29.0	6.9	11.4	18.8	0.40	0.31	7.82
53			Morris Farm	cpt1	2500	2	HF		3.5	1.6	13.5	9	28.7	7.5	12.4	13.3	0.42	0.30	0.89
54			Morris Farm	cpt3	2500	0	--		6.0	2.1	13.5	9	42.5	7.5	11.0	11.8	0.42	0.34	0.58
55			Awaroa Farm	cpt1	2500	2	HF		2.8	1.2	13.5	5	21.6	7.0	11.8	11.8	0.37	0.28	0.70
56			Keir Farm	cpt1	2500	2	HF		9.5	2.5	13.5	10	60.0	6.1	7.8	9.2	0.31	0.27	0.55
57			Sewage pumping station	cpt1	2500	3	HF		2.9	1.3	15	10	27.7	2.4	4.0	4.7	0.26	0.18	0.46
58			Edgecumbe pipe breaks	cpt1	2500	3	Indet.		5.3	2.6	13.5	10	44.7	5.3	7.7	9.0	0.39	0.27	0.55
59			Whatakane saw mill/board mill	cpt1/2	2500	1	HF		4.1	1.4	15	35	35.4	2.3	3.6	12.9	0.27	0.20	1.18
60			Whatakane Hospital	cpt2	2500	0	--		4.8	4.4	15	5	68.1	11.5	14.0	14.0	0.26	0.12	2.70
61	7.0	1989 Loma Prieta, CA	Alameda Bay Farm Island	SLR	580	2	HF	Bennett (1990);	3.0	1.8	18	10	41.7	5.9	8.7	10.2	0.27	0.18	0.91
62			Alameda Bay Farm Island	dike	580	0	--	Tuttle et al. (1990a);	4.5	2.5	18	10	61.4	27.1	34.5	40.4	0.27	0.18	3110.27
63			Clint Miller Farms	CMF1	180	0	--	Holzer et al. (1994);	4.8	3.4	18	70	72.7	1.7	2.0	7.1	0.36	0.22	0.54
64			Clint Miller Farms	CMF2	180	0	--	Mitchell et al. (1994);	5.0	6.4	18	76	103.7	2.6	2.5	9.0	0.36	0.16	0.92
65			Clint Miller Farms	CMF3	180	3	LS	Bennett & Tinsley (1995);	6.6	5.7	18	41	110.0	2.1	2.0	7.0	0.36	0.20	0.59
66			Clint Miller Farms	CMF5	180	3	LS	Boulanger et al. (1995);	5.5	4.7	18	16	91.2	3.4	3.5	6.1	0.36	0.20	0.52
67			Clint Miller Farms	CMF8	180	3	LS	Boulanger et al. (1997);	7.5	4.9	18	14	109.5	4.4	4.2	6.5	0.36	0.22	0.49
68			Clint Miller Farms	CMF10	180	0	--	Boulanger et al. (1998);	8.5	3.0	18	20	99.0	5.4	5.5	11.6	0.36	0.28	0.70
69			Clint Miller Farms	CMF12A	180	1	LS	Charlie et al. (1998);	6.1	4.6	18	35	95.1	2.5	2.5	9.0	0.36	0.21	0.70
70			Farris Farm	58	605	2	LS	Gilstrap & Youd (1998);	7.6	4.8	18	5	109.3	8.6	8.2	8.2	0.36	0.23	0.59
71			Farris Farm	59	605	2	LS	Kayen et al. (1998);	6.2	4.8	18	5	97.9	7.0	7.1	7.1	0.36	0.21	0.57
72			Farris Farm	61	605	2	LS	Mejia (1998);	8.1	4.2	18	9	107.5	7.3	7.0	7.6	0.36	0.24	0.51
73			Granite Construction Co.	123	1370	2	LS	Tinsley et al. (1998);	7.7	5.0	18	18	112.1	4.6	4.3	8.3	0.34	0.21	0.65
74			Jefferson Ranch	32	190	3	LS	Toprak et al. (1999);	2.4	1.8	18	4	37.3	2.3	3.5	3.5	0.21	0.13	0.51
75			Jefferson Ranch	34	190	1	LS	Moss (2003)	3.0	1.7	18	4	41.2	6.1	9.0	9.0	0.21	0.14	1.03
76			Jefferson Ranch	121	1410	1	HF		7.4	3.4	18	7	94.0	5.4	5.6	5.6	0.21	0.15	0.64
77			Kett	74	610	2	LS		2.7	1.5	18	15	36.8	4.6	7.1	11.7	0.40	0.27	0.71
78			Leonardini Farm	37	210	1	LS		3.6	2.5	18	13	54.0	3.4	4.5	6.5	0.21	0.13	0.84
79			Leonardini Farm	39	210	3	LS		3.4	1.9	18	11	46.5	1.5	2.1	2.6	0.21	0.14	0.35
80			Leonardini Farm	51	515	3	HF		2.9	1.8	18	8	41.4	4.0	5.9	5.9	0.21	0.14	0.74
81			Leonardini Farm	52a	515	0	--		3.3	2.7	18	12	53.5	5.9	7.9	10.7	0.21	0.12	1.45
82			Leonardini Farm	53	515	3	HF		3.5	2.1	18	6	49.3	3.7	5.1	5.1	0.21	0.14	0.64
83			Marina District	M1	120	0	--		3.0	2.3	19	2	50.1	5.5	7.5	7.5	0.17	0.10	1.24
84			Marina District	M2	120	0	--		3.0	2.7	19	3	54.1	6.3	8.4	8.4	0.17	0.09	1.48
85			Marina District	M3	120	0	--		3.0	2.7	19	3	54.1	7.1	9.6	9.6	0.17	0.09	1.68
86			Marina District	M4	120	2	HF		4.2	2.9	19	5	67.0	2.6	3.1	3.1	0.17	0.10	0.56
87			Marina District	M6	120	0	--		6.2	5.5	19	4	110.9	4.0	3.8	3.8	0.17	0.09	0.74
88			Marinovich	65	610	2	LS		5.2	5.6	19	30	102.7	2.9	2.9	8.9	0.36	0.18	0.82
89			Marinovich	67	610	0	--		6.3	6.2	18	15	112.4	14.2	13.3	21.9	0.36	0.18	44.51
90			McGowan	136	1400	0	--		2.9	2.4	18	11	47.3	3.8	5.3	6.7	0.29	0.17	0.68
91			McGowan	138	1400	0	--		3.6	1.8	18	38	47.1	2.1	3.0	10.5	0.29	0.21	0.83
92			Model Airport	18	190	3	LS		3.4	2.4	18	25	51.4	2.3	3.2	8.2	0.29	0.18	0.75
93			Model Airport	21	190	3	LS		4.1	2.4	18	6	57.1	3.8	4.9	4.9	0.29	0.19	0.45
94			ML, Sandholdt Rd	UC-4	1400	2	LS		2.5	1.8	18	2	38.1	6.6	10.1	10.1	0.25	0.15	1.06
95			ML, Sandholdt Rd	UC-5	1400	0	--		9.5	1.8	18	4	95.5	24.9	25.5	25.5	0.25	0.22	119.17
96			ML, Sandholdt Rd	UC-3	1400	1	LS		2.7	1.7	18	4	38.8	7.0	10.6	10.6	0.25	0.16	1.06
97			ML, Sandholdt Rd	RC-1	n/a	1	LS		1.4	1.4	18	4	25.2	3.0	5.1	5.1	0.25	0.13	0.67
98			ML, Sandholdt Rd	UC-2	1400	0	--		1.9	1.7	18	4	32.2	10.4	16.7	16.7	0.25	0.14	6.83
99			ML, Sandholdt Rd	RC-4	n/a	2	LS		5.0	1.8	18	1	58.6	8.0	10.4	10.4	0.25	0.20	0.86
100			ML, Sandholdt Rd	UC-6	1400	0	--		6.5	1.7	18	1	69.9	18.2	21.9	21.9	0.25	0.21	38.08
101			ML, MBARI No. 3	RC-5	n/a	0	--		3.5	1.8	18	1	46.3	15.5	22.1	22.1	0.25	0.18	49.69
102			ML, MBARI No. 3	RC-6	n/a	0	--		4.1	2.6	18	1	59.1	13.0	16.8	16.8	0.25	0.16	6.30
103			ML, MBARI No. 3	RC-7	n/a	0	--		4.7	3.7	18	1	74.8	9.2	10.7	10.7	0.25	0.14	1.20
104			ML, MBARI Tech Bldg	RC-9	n/a	0	--		3.5	2.0	18	4	48.3	12.4	17.4	17.4	0.25	0.17	7.79
105			ML, MBARI No. 4	CPT-1	n/a	0	--		3.4	1.9	18	4	46.5	8.5	12.1	12.1	0.25	0.17	1.21

Case No.	Eq. M	Earthquake	Site	CPT No.	days after eq.	Liq. Severity	Failure Mech.	Reference	depth (m)	gwt depth (m)	$\gamma_{tot}$ (kN/m <sup>3</sup> )	F.C. %	$\sigma'_v$ (kPa)	$q_c$ (MPa)	$q_{c1}$ (MPa)	$(q_{c1})_{cs}$ (MPa)	$a_{max}$ (g)	CSR (MPa)	$FS_{liq}$
106			ML, MBARI No. 4	CPT-2	n/a	0	--		2.5	1.8	18	4	38.1	10.4	15.8	15.8	0.25	0.15	4.25
107			ML, MBARI No. 4	CPT-3	n/a	0	--		4.1	2.3	18	4	56.1	9.4	12.4	12.4	0.25	0.17	1.29
108			ML, MBARI No. 4	CPT-4	n/a	0	--		1.9	1.5	18	4	30.3	8.4	13.7	13.7	0.25	0.15	1.98
109			ML, General Fisheries	CPT-5	n/a	2	LS		2.1	1.5	18	4	31.9	2.5	4.0	4.0	0.25	0.15	0.46
110			ML, General Fisheries	CPT-6	n/a	0	--		2.6	1.7	18	4	38.0	10.0	15.3	15.3	0.25	0.16	3.17
111			ML, State Beach Access Rd	UC-14	1400	3	LS		3.0	1.8	18	1	42.2	3.8	5.6	5.6	0.25	0.17	0.58
112			ML, State Beach Access Rd	UC-15	1400	3	LS		3.0	1.8	18	1	42.2	3.0	4.4	4.4	0.25	0.17	0.47
113			ML, State Beach Access Rd	UC-16	1400	2	LS		2.3	2.3	18	1	41.4	6.6	9.8	9.8	0.25	0.13	1.22
114			ML, State Beach Access Rd	UC-17	1400	2	LS		4.4	2.6	18	1	61.5	5.4	6.9	6.9	0.25	0.17	0.69
115			ML, State Beach Access Rd	UC-18	1400	0	--		4.0	3.4	18	1	66.1	16.4	20.2	20.2	0.25	0.14	30.92
116			ML, Harbor Office	UC-19	1400	1	HF		6.4	3.1	18	10	82.8	7.6	8.4	9.8	0.25	0.18	0.91
117			ML, Harbor Office	UC-20	1400	2	LS		4.7	2.8	18	10	66.0	4.1	5.1	5.9	0.25	0.16	0.62
118			ML, Harbor Office	UC-21	1400	2	LS		4.2	2.7	18	10	60.9	4.9	6.3	7.3	0.25	0.16	0.76
119			ML, Harbor Office	UC-12	1400	1	LS		4.1	1.9	18	14	52.2	6.2	8.4	13.1	0.25	0.18	1.36
120			ML, Harbor Office	UC-13	1400	1	LS		4.1	1.9	18	14	52.2	4.3	5.9	9.1	0.25	0.18	0.81
121			ML, Woodward Marine	14B	190	0	--		3.6	1.2	18	3	41.3	14.4	21.4	21.4	0.25	0.20	33.38
122			ML, Woodward Marine	15A	190	2	LS		2.9	1.3	18	2	36.5	6.3	9.7	9.7	0.25	0.19	0.85
123			ML, Woodward Marine	UC-11	1400	2	LS		2.2	1.0	18	15	27.8	3.1	5.2	8.5	0.25	0.19	0.75
124			ML, Marine Laboratory	C2	90	1	LS		3.6	2.2	18	3	51.1	8.3	11.4	11.4	0.25	0.16	1.15
125			ML, Marine Laboratory	C3	90	3	LS		4.4	1.5	18	3	50.8	6.8	9.4	9.4	0.25	0.20	0.76
126			ML, Marine Laboratory	C4	90	3	LS		5.5	2.8	18	3	72.5	1.9	2.2	2.2	0.25	0.17	0.26
127			Port of Oakland	POO-2	580	3	LS		6.5	2.3	18	3	75.8	4.7	5.4	5.4	0.29	0.23	0.41
128			Port of Oakland	POO-3	580	2	LS		5.7	2.3	18	2	69.2	5.9	7.1	7.1	0.29	0.22	0.54
129			Port of Richmond	POR-2	580	1	HF		6.5	2.5	18	51	77.8	1.8	2.0	7.2	0.16	0.12	0.98
130			Port of Richmond	POR-3	580	2	HF		6.3	2.5	18	30	76.1	2.3	2.7	8.2	0.16	0.12	1.12
131			Oakland Intl Airport	ACPT7	580	3	LS		2.7	2.0	18	5	41.7	2.1	3.2	3.2	0.27	0.16	0.36
132			San Fran-Oakland Bay Bridge	SFOBB1	580	3	HF		6.5	2.0	18	12	72.9	3.8	4.5	6.1	0.29	0.23	0.44
133			San Fran-Oakland Bay Bridge	SFOBB2	580	3	HF		7.6	2.0	18	12	81.9	5.9	6.5	8.9	0.29	0.24	0.60
134			San Fran-Oakland Bay Bridge	SFOBB5	580	3	HF		7.4	2.0	18	12	80.2	3.2	3.6	4.9	0.29	0.24	0.36
135			Radovich Farm	RAD98	630	0	--		3.9	3.5	18	15	66.3	6.7	8.2	13.6	0.36	0.20	1.42
136			Radovich Farm	RAD99	630	2	HF		5.0	4.1	18	9	81.2	5.0	5.6	6.0	0.36	0.20	0.50
137			Scattini	SCA23	190	0	--		4.0	1.5	18	32	47.5	2.0	2.8	9.2	0.23	0.18	0.84
138			Scattini	SCA28	190	2	LS		3.6	1.2	18	3	41.3	3.6	5.3	5.3	0.23	0.19	0.49
139			Sea Mist	SEA31	190	3	LS		3.2	1.9	18	29	44.8	0.8	1.2	3.6	0.22	0.15	0.45
140			Pajaro Dunes	PD1-43	300	0	--		3.6	2.6	18	19	55.0	5.8	7.7	15.6	0.22	0.13	4.40
141			Pajaro Dunes	PD1-44	300	2	LS		4.4	3.4	18	5	69.4	5.4	6.6	6.6	0.22	0.13	0.85
142			Pajaro Dunes	PD2a-79	300	0	--		2.5	1.5	18	1	35.2	10.9	17.0	17.0	0.22	0.15	7.49
143			Southern Pacific RR bridge	SPR48	300	2	LS		6.4	5.3	18	13	104.4	2.9	2.9	4.2	0.33	0.18	0.40
144			Watsonville Municipal Airport	WAT54	300	0	--		9.9	8.2	18	13	161.5	15.0	11.2	16.3	0.40	0.21	3.69
145			Silliman Farm	SIL68	610	2	LS		6.2	3.5	18	15	85.1	4.4	4.8	7.9	0.38	0.25	0.51
146			Silliman Farm	SCR89	610	0	--		4.6	3.4	18	8	71.0	6.1	7.2	7.2	0.40	0.24	0.50
147			Tanimura	TAN103	680	2	LS		9.0	4.6	18	13	118.8	3.6	3.2	4.7	0.14	0.09	0.87
148			Tanimura	TAN105	680	0	--		5.3	4.2	18	33	84.6	3.4	3.7	12.3	0.14	0.08	2.64
149			Martella	MAR110	710	0	--		3.7	1.8	18	13	48.0	3.1	4.4	6.4	0.13	0.09	1.16
150			Martella	MAR111	710	0	--		2.1	1.7	18	19	33.9	2.5	4.0	8.0	0.13	0.08	1.74
151			Salinas River Bridge	SRB116	n/a	0	--		6.6	6.4	18	7	116.8	4.0	3.6	3.6	0.11	0.06	1.17
152			Salinas River Bridge	SRB117	n/a	0	--		6.5	6.4	18	13	116.0	4.2	3.8	5.6	0.11	0.06	1.72
153	6.1	1992 Bay of Plenty, New Zealand	Robinson Farm east	cpt1	2500	0	--	Christensen (1995)	3.6	0.8	13.5	7	20.7	3.5	6.0	6.0	0.08	0.06	1.57
154			Robinson Farm west	cpt4	2500	0	--		1.8	0.6	13.5	7	12.6	3.7	6.3	6.3	0.08	0.05	1.98
155	6.7	1994 Northridge, CA	Balboa Blvd	Bal-10	450	2	LS	Bennett et al. (1998);	8.3	7.2	18.5	36	142.8	3.5	2.8	10.1	0.84	0.39	0.41
156			Wynne Ave.	Wyn-1	440	1	LS	Toprak et al. (1999);	7.8	4.7	18.5	16	113.9	4.9	4.6	7.9	0.51	0.28	0.46
157			Wynne Ave.	Wyn-5a	445	2	LS	Holzer et al. (1999)	7.6	4.3	18.5	31	108.2	4.1	3.9	12.4	0.51	0.29	0.74
158			Potrero Canyon	Pot-3	480	2	LS		5.2	3.3	18.5	79	77.6	2.8	3.2	11.3	0.43	0.24	0.77
159			Potrero Canyon	Pot-8	480	2	LS		6.0	3.3	18.5	52	84.5	2.9	3.1	11.1	0.43	0.25	0.72

Case No.	Eq. M	Earthquake	Site	CPT No.	days after eq.	Liq. Severity	Failure Mech.	Reference	depth (m)	gwt depth (m)	$\gamma_{tot}$ (kN/m <sup>3</sup> )	F.C. %	$\sigma'_v$ (kPa)	$q_c$ (MPa)	$q_{c1}$ (MPa)	$(q_{c1})_{cs}$ (MPa)	$a_{max}$ (g)	CSR (MPa)	$FS_{liq}$
160	6.9	1995 Kobe, Japan	Fukuzumi Park	FUP-1	n/a	0	--	Hamada et al. (1996);	11.6	3.1	19	6	137.0	16.1	13.4	13.4	0.55	0.39	0.68
161			Honijo Central Park	HCP-1	n/a	0	--	Shibata et al. (1996); Cetin	5.0	2.5	19	6	70.5	14.2	17.0	17.0	0.50	0.33	3.30
162			Kobe Art Institute	KAI-2	n/a	0	--	et al. (2000); Moss (2003);	3.7	3.0	19	5	63.4	11.4	14.3	14.3	0.34	0.19	1.89
163			Sumiyoshi Elementary School	SES-1	n/a	0	--	Suzuki et al. (2003)	2.8	1.9	19	0	44.4	10.3	14.9	14.9	0.60	0.36	1.23
164	7.6	1999 Chi-Chi, Taiwan	Wufeng	WF-C7	120	3	BC/HF	Stewart (2001);	6.9	3.2	19	40	94.8	1.6	1.7	5.9	0.67	0.59	0.17
165			Wufeng	WF-C8	90	0	--	Juang et al. (2002, 2005);	9.2	0.5	19	44	89.5	6.4	6.8	24.0	0.67	0.82	19.94
166			Wufeng (Site M)	WF-C9	90	3	LS	Yuan et al. (2003);	3.0	2.0	19	49	47.2	1.0	1.4	5.0	0.67	0.53	0.16
167			Wufeng	WF-C10	90	3	LS	Ku et al. (2004);	6.4	4.0	19	22	98.1	2.2	2.3	5.2	0.67	0.53	0.17
168			Wufeng	WAC-2	730	0	--	Chu et al. (2004, 2006);	6.9	1.1	19	23	74.2	6.0	7.0	16.8	0.67	0.76	1.35
169			Wufeng (Site B)	WBC-2	730	3	LS	Juang (2002, online);	3.5	1.5	19	19	46.9	2.0	2.9	5.9	0.67	0.63	0.16
170			Wufeng (Site C)	WCC-2	730	3	LS	Stewart et al. (2003,online)	3.0	1.2	19	21	39.3	4.0	6.0	13.4	0.67	0.64	0.41
171			Wufeng (Site C)	WCC-6	1030	3	LS		3.0	1.2	19	13	39.3	2.2	3.3	4.8	0.67	0.64	0.13
172			Wufeng	WEC-1	1030	2	LS		6.0	1.0	19	14	65.0	5.0	6.2	9.6	0.67	0.76	0.21
173			Yualin	YL-C2	60	1	HF		3.2	0.6	19	18	35.3	2.5	3.9	7.5	0.18	0.20	0.61
174			Yualin	YL-C3	60	0	--		10.0	1.8	19	15	109.6	7.0	6.6	10.9	0.18	0.19	0.93
175			Yualin	YL-C4	60	2	Indet.		5.8	0.7	19	49	60.2	2.1	2.7	9.7	0.18	0.21	0.74
176			Yualin	YL-C6	90	1	Indet.		3.8	1.8	19	70	52.6	2.1	2.8	9.9	0.18	0.16	0.99
177			Yualin	YL-C15	45	0	--		9.8	0.9	19	50	98.4	4.4	4.4	15.7	0.18	0.21	2.88
178			Yualin	YL-C16	60	0	--		5.9	2.5	19	33	78.7	2.6	2.9	9.8	0.18	0.17	0.96
179			Yualin	YL-C32	45	2	Indet.		5.8	0.7	19	51	60.2	1.6	2.1	7.5	0.18	0.21	0.58
180			Yualin	YL-C21	55	1	Indet.		7.0	1.7	19	19	81.0	5.2	5.8	11.7	0.18	0.19	1.03
181			Yualin	YL-C22	45	3	HF		4.0	1.1	19	17	47.6	2.3	3.2	6.0	0.18	0.19	0.54
182			Yualin	YL-C24	55	3	HF		3.4	2.0	19	15	50.9	2.5	3.4	5.7	0.18	0.15	0.64
183			Yualin	YL-C43	60	2	HF		2.9	2.3	19	90	49.2	1.4	2.0	7.1	0.18	0.13	0.88
184			Yualin	YL-C25	50	1	Indet.		3.0	2.3	19	30	50.1	2.3	3.2	9.9	0.18	0.14	1.19
185			Yualin	YL-C20	45	1	Indet.		6.1	1.8	19	30	73.7	2.1	2.4	7.4	0.18	0.18	0.67
186			Yualin	YL-C19	45	2	HF		5.0	0.8	19	57	53.8	2.1	2.9	10.2	0.18	0.21	0.80
187			Yualin	YL-C26	50	1	Indet.		13.0	2.3	19	17	142.0	5.5	4.5	8.2	0.18	0.17	0.77
188			Yualin	YL-C45	60	1	Indet.		4.8	2.3	19	19	66.7	2.7	3.3	6.7	0.18	0.16	0.70
189			Nantou	NT-C7	90	3	HF		4.1	3.6	19	42	73.0	0.9	1.1	3.8	0.43	0.30	0.23
190			Nantou	NT-C15	130	2	HF		6.6	3.4	19	6	94.0	4.9	5.1	5.1	0.43	0.37	0.24
191			Nantou	NT-C11	90	1	Indet.		2.5	1.8	19	76	40.6	2.7	4.1	14.5	0.43	0.33	1.13
192			Nantou	NAC-1	375	0	--		2.8	1.0	19	80	35.5	1.4	2.1	7.5	0.43	0.43	0.29
193			Nantou (Site N)	NCC-3	375	2	LS		2.7	1.0	19	10	34.6	2.0	3.2	3.7	0.43	0.42	0.16
194	7.4	1999 Kocaeli (Izmit), Turkey	Building Site H	CPT-H2	335	3	HF	Bray et al. (2000, online);	2.4	1.7	19	15	38.7	3.3	5.0	8.2	0.40	0.29	0.47
195			Hotel Sapanca	SH-2	365	3	LS	Bray et al. (2003);	4.8	1.1	19	9	54.9	6.3	8.4	9.0	0.40	0.40	0.37
196			Hotel Sapanca	SH-7	365	3	LS	Cetin et al. (2002, 2004);	5.7	1.1	19	10	62.7	4.8	6.1	7.1	0.40	0.41	0.29
197			Hotel Sapanca	SH-9	365	3	LS	Kanatani et al. (2003);	5.8	2.6	19	15	78.8	2.1	2.4	3.9	0.40	0.33	0.21
198			Hotel Sapanca	SH-11	365	3	LS		4.3	1.4	19	10	53.3	2.9	4.0	4.6	0.40	0.37	0.22
199			Cumhuriyet Cadessi	4-22	325	0	--		2.7	1.0	19	72	34.6	2.5	4.0	14.0	0.40	0.36	0.89
200			Police Station	PS-3	370	3	LS		2.5	1.2	19	36	34.7	1.4	2.2	8.0	0.40	0.34	0.39
201			Police Station	PS-4	370	3	LS		2.5	1.2	19	78	34.7	1.7	2.6	9.3	0.40	0.34	0.45
202			Soccer Field	SF-5	370	3	LS		1.5	1.0	19	16	23.6	2.9	5.0	8.7	0.40	0.30	0.48
203			Soccer Field	SF-6	370	3	LS		1.5	1.0	19	52	23.6	1.0	1.8	6.3	0.40	0.30	0.35
204			Yalova Harbor	YH-3	380	2	LS		3.7	0.8	19	9	41.4	4.1	6.1	6.5	0.30	0.31	0.35
205			Yalova Harbor	YH-4	380	2	LS		3.5	0.8	19	13	40.0	2.8	4.2	6.1	0.30	0.30	0.34
206			Yakin Cadessa	A1	300	2	LS		4.2	0.8	19	93	46.0	2.9	4.1	14.7	0.40	0.42	0.97

Notes: 1. Liquefaction severity: 0 = No liquefaction; 1 = marginal liquefaction; 2 = moderate liquefaction; 3 = severe liquefaction.

2. Failure mechanism: HF = hydraulic fracture; LS = lateral spread; Indet. = indeterminate.

**Table 2. Potential combinations of log cycles of time elapsed between earthquake triggering liquefaction and time when in situ penetration resistance data are collected**

Time after earthquake required for reconsolidation, $t_{95}$ (days)	$t_{\text{elapsed,avg}}$ (days)	$\log_{10}(t_{\text{elapsed,avg}}/t_{95})$	$t_{\text{elapsed,max}}$ (days)	$\log_{10}(t_{\text{elapsed,max}}/t_{95})$	$t_{\text{elapsed,min}}$ (days)	$\log_{10}(t_{\text{elapsed,min}}/t_{95})$
1	1030	3.0	7050	3.8	45	1.7
7		2.2		3.0		0.8
14		1.9		2.7		0.5

In summary, because much of the penetration resistance data used to construct liquefaction resistance relationships (such as those shown in Figure 2) were collected some time after the causative earthquake, a significant portion of the potential post-earthquake aging effects may already be reflected in the measured penetration resistances. As a result, in some Holocene settings, it may be of secondary importance to correct the penetration resistance data for potential post-liquefaction aging effects. However, this effect still should be considered on a case-by-case basis.

Following early work by Christian and Swiger (1975), Haldar and Tang (1979), and Liao et al. (1988), considerable work has been done in the decade to apply various probability theories and statistical methods to liquefaction analysis. Investigators have used Bayesian analysis (e.g., Juang et al. 2000; Cetin et al. 2004a; Moss et al. 2006); logistic and other regression analyses (e.g., Youd and Noble 1997; Toprak et al. 1999; Hwang and Yang 2001); reliability-based methods (e.g., first-order reliability method) (Juang et al. 1999; Juang et al. 2006); and other techniques to assess the uncertainties associated with liquefaction triggering. While these studies have used different approaches to evaluate the probability of liquefaction occurring, they have one primary aspect that is identical – they have treated all of the liquefaction data points in the same manner. That is, they consider all of the records to have equal weight and do not consider the potential effect of the severity of liquefaction implied by the manifestations of liquefaction (i.e., the size, number, and distribution of liquefaction features). Only Cetin et al. (2004) considered weighting the liquefaction data slightly more than the no liquefaction data, but they did not use this weighted method in their recommended approach. Table 3 presents definitions of liquefaction severity proposed by Olson et al. (2005)/Green et al. (2005) and Bray et al. (2000)/Juang et al (2005). We used a combination of both definitions to classify liquefaction severity for each case record.

To examine the importance of the severity of liquefaction on liquefaction resistance, we collected the data in Table 1 based on the following criteria:

1. Each CPT sounding was performed in proximity to a boring with SPT blow count was measured in order to confirm stratigraphy and provide a sample where fines content was measured.
2. A reasonable estimate of liquefaction severity could be discerned from published reports and descriptions of the site.

**Table 3. Liquefaction severity definitions proposed by various investigators**

Olson et al. (2005)/Green et al. (2005)		Bray et al. (2000)/Juang et al. (2005)	
Category	Description	Category	Description
No liquefaction	<ul style="list-style-type: none"> <li>No sand blows</li> <li>No lateral spreading features</li> <li>No subvertical sand dikes</li> <li>Possible subhorizontal sand sills</li> </ul>	No observed ground damage	<ul style="list-style-type: none"> <li>No settlement</li> <li>No building tilt</li> <li>No lateral movement</li> <li>No sand boils</li> </ul>
Marginal liquefaction	<ul style="list-style-type: none"> <li>Effects that are barely discernable (e.g., cracking of cap at ground surface) or weakly developed (e.g., scattered small sand blows)</li> </ul>	Minor to moderate damage	<ul style="list-style-type: none"> <li>Settlement &lt; 25 cm</li> <li>Building tilt &lt; 3°</li> <li>Lateral movement &lt; 10 cm</li> </ul>
Moderate liquefaction	<ul style="list-style-type: none"> <li>Lateral spreads with dikes ~ 15 cm in width</li> <li>Scattered large sand blows</li> </ul>	Major ground damage	<ul style="list-style-type: none"> <li>Settlement ≥ 25 cm</li> <li>Building tilt ≥ 3°</li> <li>Lateral movement ≥ 10 cm</li> <li>Building collapse</li> </ul>
Severe liquefaction	<ul style="list-style-type: none"> <li>Dikes ~ 0.5 m wide or larger</li> <li>Numerous large sand blows</li> <li>Severe warping or distortion of ground surface or of thick fine-grained strata at depth</li> </ul>		

One of the primary differences between this database and others is that we intentionally included more than one sounding per liquefaction site depending on the details available in the literature. For example, if the boundaries of a lateral spread were clearly delineated by investigators and soundings were performed both inside and outside of the sliding mass, we included both of the soundings in the database – and we assigned each a different liquefaction severity classification.

Figure 6 presents the case records detailed in Table 1, plotted in terms of clean sand normalized tip resistance,  $(q_{cl})_{cs}$ . We used the fines content adjustment proposed by Newman (2007) to adjust  $q_{cl}$  to  $(q_{cl})_{cs}$  in evaluating these cases. Careful examination of Figure 6 clearly indicates that the severity of liquefaction affects the proximity of the data points to the clean sand liquefaction resistance boundary curve, with marginal liquefaction cases generally plotting nearest to the clean sand boundary curve.

Figure 7 presents histograms and statistics of factor of safety against level-ground liquefaction ( $FS_{liq}$ ) based on the severity of liquefaction, where  $FS_{liq}$  is defined in Eq. (4). As illustrated in Figure 7, the  $FS_{liq}$  clearly and systematically decreases as the observed liquefaction effects become more severe. Previous paleoliquefaction studies that employ the cyclic stress method have assumed that  $FS_{liq}$  in Eq. (5) equals unity in order to estimate  $a_{max}$ . However, this assumption always yields a strength of shaking that is less than or equal to the actual strength of shaking (i.e., underestimates the size of the paleoearthquake). Using a  $FS_{liq}$  in Eq. (5) that properly reflects the observed severity of liquefaction should yield a reasonable estimate of the strength of shaking (i.e., paleoearthquake magnitude) for a much wider range of conditions. The one exception is for cases of no liquefaction. Because the  $FS_{liq}$  for sites that do not liquefy can theoretically range from unity to infinity, it was not possible to define reasonable statistics (i.e., mean and standard deviation) for cases of no liquefaction.

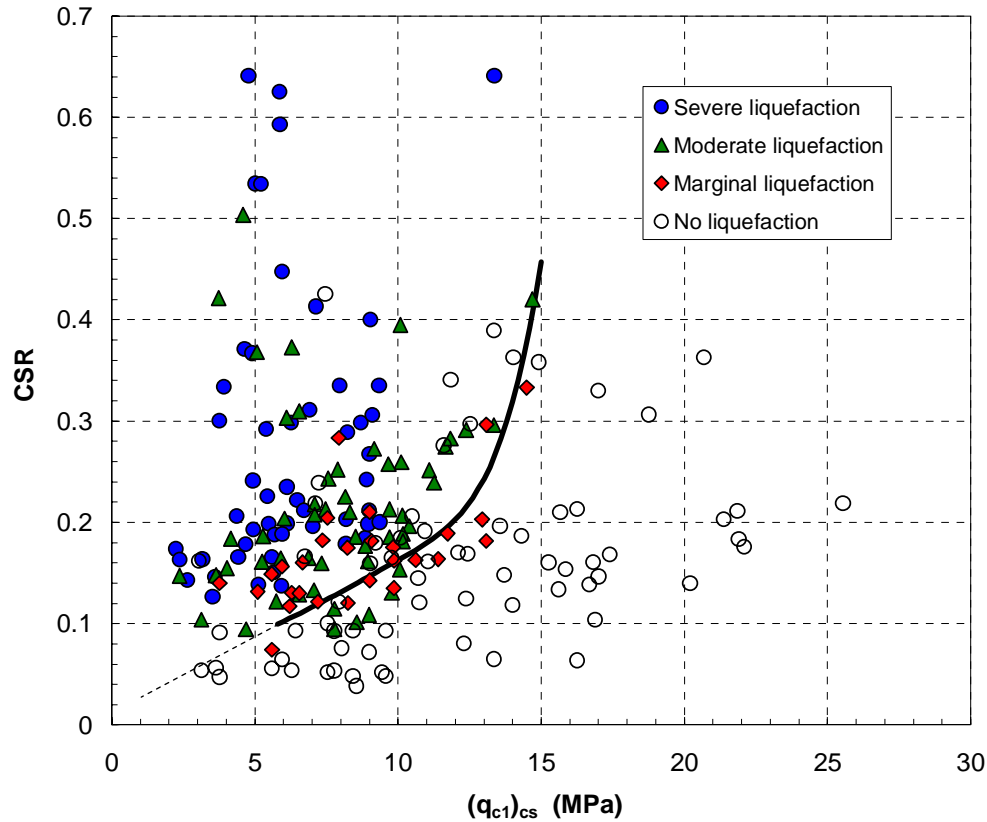


**Figure 6. Liquefaction/no liquefaction case records compared to clean sand liquefaction resistance relationship from Olson and Stark (1998) and Newman (2007).**

As discussed above, the fines content (FC) adjustment and overburden correction factor ( $K_{\sigma}$ ) are two other uncertain parameters that affect liquefaction resistance. For this study, we address the epistemic uncertainties in these factors by utilizing multiple models that are weighted based on expert opinion as presented in Table 4. Aleatoric uncertainties are indirectly treated by using random variables for the inputs to these adjustments, i.e., fines content and vertical effective stress.

**Table 4. Uncertainties related to liquefaction resistance resulting from fines content adjustment and overburden stress correction**

Factor	Model	Weight
FC adjustment	Kayen and Mitchell (1997)	0.25
	Youd et al. (2001)	0.25
	Cetin et al. (2004)	0.25
	Idriss and Boulanger (2006)	0.25
Overburden stress correction, $K_{\sigma}$	Seed and Harder (1990)	0.1
	Harder and Boulanger (1997)	0.1
	Youd et al. (2001)	0.5
	Idriss and Boulanger (2006)	0.3

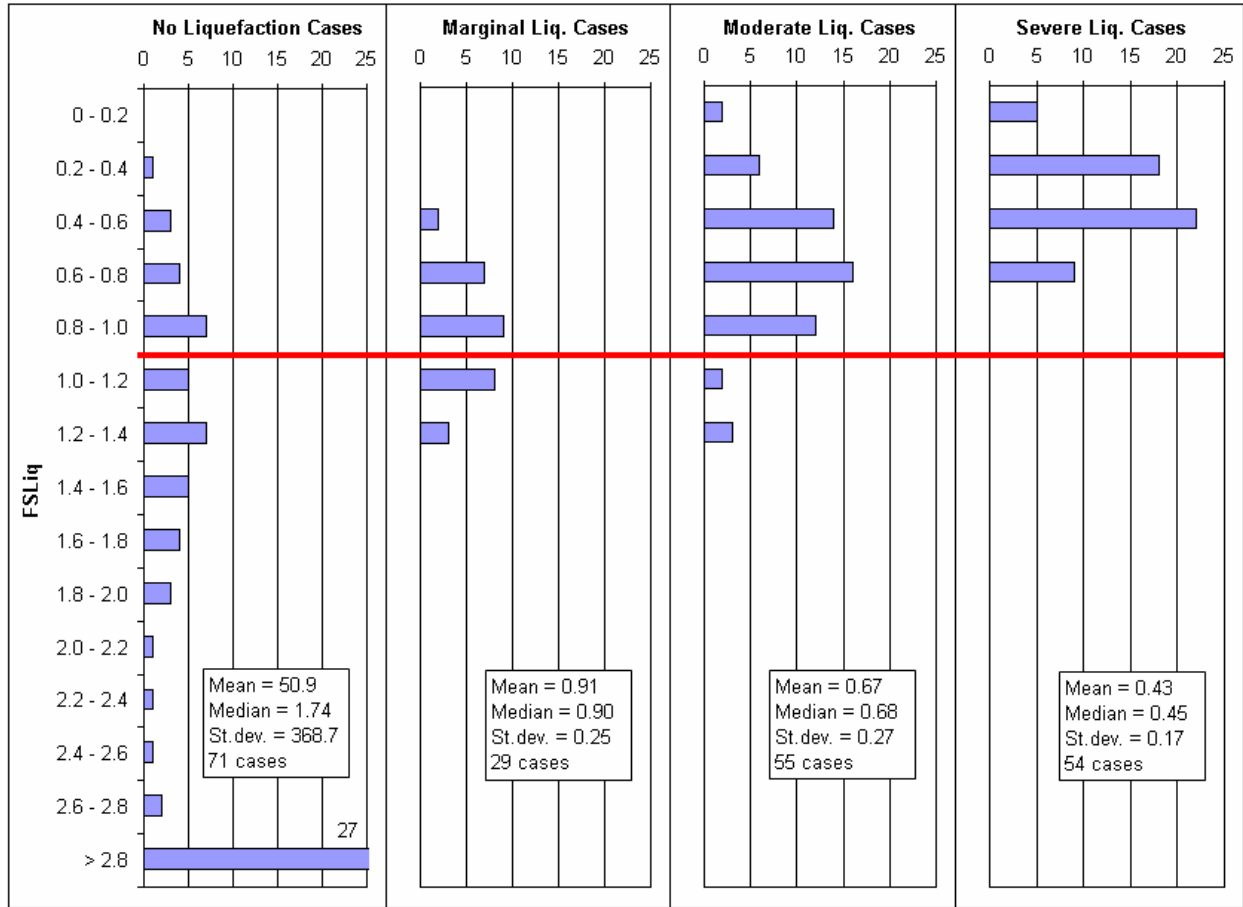


**Figure 7. Histograms and statistics of factor of safety against liquefaction for various liquefaction severities (no liquefaction, marginal liquefaction, moderate liquefaction, and severe liquefaction).**

### Treating field observations, ground failure mechanism, and field setting

The primary ground failure mechanisms that can lead to the emplacement of seismic liquefaction features include hydraulic fracturing, lateral spreading, and surface oscillation. However, other mechanisms such as a bearing capacity failure of an overlying structure can cause ground rupture and create a conduit for relieving seismically-induced excess porewater pressures and emplacing sand dikes. Table 1 includes the likely mechanism that was chiefly responsible for ground failure at each of the liquefaction sites, and Figure 8 plots these data with respect to the Olson and Stark (1998)/Newman (2007) clean sand liquefaction resistance boundary curve. The data in Figure 8 are classified in terms of the likely failure mechanism. As illustrated in the figure, there are no discernible systematic differences in the position of the data based on the failure mechanism. In other words, sites that experienced hydraulic fracturing have similar maximum and minimum factors of safety against level-ground liquefaction as sites that experienced lateral spreading.

As a result, we anticipate that the ground failure mechanism has (at most) a secondary effect on the back-calculated strength of shaking. Therefore, we ignored this potential effect in our back-analyses.

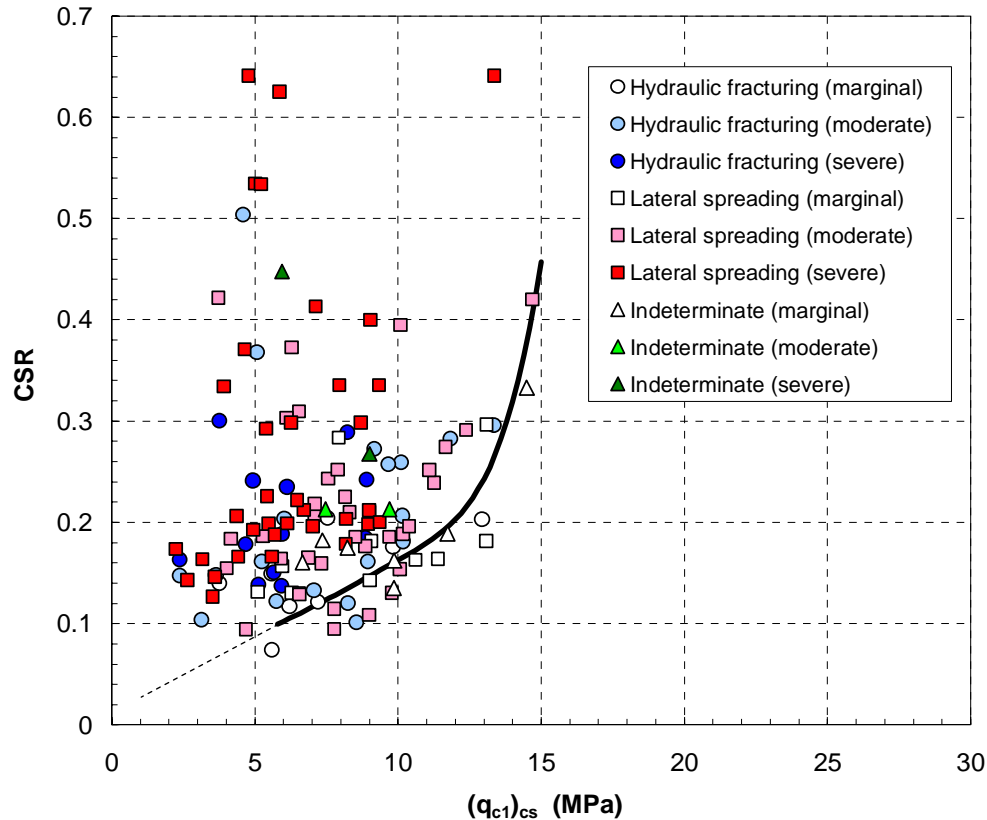


**Figure 8. Liquefaction case records compared to clean sand liquefaction resistance relationship from Olson and Stark (1998) and Newman (2007) (no liquefaction cases are not included in the figure). The liquefaction data are classified in terms of both likely failure mechanism and liquefaction severity. Cases classified as indeterminate likely include some cases of surface oscillation.**

It is impossible to quantify the potential combinations of field observations that can result from a thorough paleoliquefaction field investigation. Therefore, Green et al. (2005) proposed a ‘field data quality’ (FDQ) index to subjectively rank (using the classifications of high, intermediate, or low) the quality of and confidence in geologic interpretations at an individual study site. The FDQ should incorporate the following factors: (1) variability of geologic setting (e.g., braid-bar, point bar, etc.); (2) depth of potential source beds at the time of the earthquake; (3) depth of the groundwater table at the time of the earthquake; (4) mechanism of ground failure (e.g., hydraulic fracturing, lateral spreading, surface oscillation); and (5) severity of liquefaction, as it relates to making proper field interpretations. In turn, the quality of and confidence in the geologic interpretations are influenced by a number of factors, including the number, spacing, and locations of in situ borings or tests; the vertical and lateral variability of sediments at the site; the method of observation (i.e., plan view versus sectional view); and the length and quality of the bank exposure at the site. These factors are qualitatively combined to assess the overall FDQ of an individual study site.

The infinite number of potential combinations for field observations that influence FDQ does not make FDQ amenable to direct statistical analysis. However, to indirectly account for FDQ, we propose to use the FDQ ranking to quantify the coefficients of variation (COV) for the random variables that are employed in the back-analysis. Table 5 summarizes the typical ranges of COV

published in the literature for various parameters used in a paleoliquefaction back-analysis, as well as the recommended COV values associated with random variables based on FDQ rankings.

**Table 5. Coefficients of variation (COV) associated with random variables based on FDQ rankings. The COV values account for both aleatory and epistemic uncertainty where available. All COV values in percent.**

Variable	Reported COV range (mean)	References	COV assigned to FDQ ranking		
			High	Intermediate	Low
Unit weight (kN/m <sup>3</sup> )	3 – 20 (9) 3 – 7 (--) 0 – 10 (--) <sup>(1)</sup>	Phoon and Kulhawy (1999) Kulhawy (1992); Duncan (2000) Lacasse and Nadim (1996)	5	10	15
Fines content (%)	1 – 43 (20) <sup>(2)</sup> 9 – 70 (25) <sup>(3)</sup>	Baecher and Christian (2003) Baecher and Christian (2003)	15	25	35
Measured N-value	26 (--) 14 – 100 (15 – 45) 19 – 62 (54) <sup>(3)</sup> 25 – 50 (--)	Harr (1987) Kulhawy and Trautmann (1996) Phoon and Kulhawy (1999) Baecher and Christian (2003)	25	35	45
Measured q <sub>c</sub> -value	37 (--) 8 – 22 (5 – 15) 10 – 81 (38) <sup>(4)</sup> 20 – 60 (--)	Harr (1987) Kulhawy and Trautmann (1996) Phoon and Kulhawy (1999) Baecher and Christian (2003)	15	25	35

Notes: (1) Reported values for buoyant unit weight  
(2) Reported values for sand content.  
(3) Reported values for clay content.  
(4) Reported values for tests performed in sand.

In addition to these random variables, the FDQ factor also considers the depth to liquefaction (or source bed) and the water table depth (at the time of the earthquake). The potential ranges for these values will be based solely on field observations and interpretations (e.g., Obermeier et al. 2001, 2005). However, statistics such as mean and standard deviations are difficult to define, because field observations almost exclusively provide only best estimates and upper and lower bounds for these variables. Therefore, rather than using statistical rules to estimate the mean and standard deviations of these variables, we recommend using simplified approaches (that assume a normal distribution) such as the 3σ approximation (Dai and Wang 1992; Duncan 2000; Jones et al. 2002). The simplified approximation uses the observation that over 99.7% of all values (of a normally distributed variable) fall within the mean (μ) ± 3 standard deviations (σ). Therefore, the standard deviation of a normally distributed variable can be estimated as:

$$\sigma = \frac{\text{Upper bound value} - \text{Lower bound value}}{6} \quad [6]$$

### Treating seismicity and seismic demand

The primary uncertainties related to seismicity and seismic demand are MSF, r<sub>d</sub>, bedrock attenuation, and site response effects. To a large extent, we treat these uncertainties using logic trees. That is, we account for the epistemic uncertainties in MSF, r<sub>d</sub>, and bedrock attenuation by weighting and combining a number of models available in the literature. Table 6 presents the models used for this study.

Rodriguez-Marek et al. (2001) evaluated the effect of site response analysis on ground motion uncertainties in proposing alternative soil classifications and amplification factors. Their results indicate that ground motion uncertainties actually decrease slightly after performing site response analyses, therefore, ground motion uncertainties estimated from bedrock attenuation relationships can conservatively be assumed to apply to the ground surface. Based on this work, we assumed that surface ground motion aleatoric uncertainties are equal to the bedrock ground motion aleatoric uncertainties. The epistemic uncertainties also are carried through simply by multiplying the mean bedrock ground motion by the 2001 NEHRP-recommended site amplification factors.

**Table 6. Uncertainties related to seismicity and seismic demand**

<b>Factor</b>	<b>Model</b>	<b>Weight</b>	<b>Comment</b>
MSF	Seed and Idriss (1982)	0.20	Initial estimates of weight based on particular model's use in practice.
	Youd and Noble (1997) ( $P_L = 50\%$ )	0.10	
	Andrus and Stokoe (1997)	0.35	
	Idriss (1999)	0.35	
$r_d$	Youd et al. (2001)	0.75	Initial estimates of weight based on particular model's use in practice.
	Iwasaki et al. (1978)	0.25	
Bedrock attenuation	Atkinson and Boore (1995)	0.25	Attenuation relationships and weighting factors taken as identical to those used by the USGS in the 2001 U.S. seismic hazard maps. Aleatoric uncertainties estimated by individual investigators.
	Frankel et al. (1996)	0.25	
	Toro et al. (1997)	0.25	
	Somerville et al. (2001)	0.125	
	Campbell (2003, 2004)	0.125	

### **Treating in situ testing**

Numerous methods are available for evaluating the uncertainties involved in various in situ testing and interpretation. In particular, geostatistics (reference) has seen increased use in the last decade. However, based on our experience, it is extremely unusual for a sufficiently large in situ data set to be collected at a paleoliquefaction site in order to perform a meaningful geostatistical analysis. As such, we decided that it was more prudent to recommend an approach that could be more widely used in paleoliquefaction back-analyses.

As discussed above, we recommend using the field data quality (FDQ) factor to capture the aleatoric and epistemic uncertainties involved in characterizing individual paleoliquefaction sites. Table 5 provides our recommendations for coefficients of variation for the most commonly used penetration tests used to characterize paleoliquefaction sites. These can be used in conjunction with the representative value of penetration resistance defined using the Olson et al. (2005a) recommendations. For convenience, we repeat those recommendations in Table 7.

### **Treating the magnitude bound method**

The primary uncertainties in developing a regional magnitude bound for use in paleoliquefaction analysis are estimating the magnitudes of pre-instrumental earthquakes in the region and estimating the site-to-source distances for the most distal liquefaction sites caused by those paleoearthquakes.

**Table 7. Guidelines for selecting a representative penetration resistance value (Olson et al. 2005a)**

Ground failure mechanism	Sectional view observations of marginal liquefaction	Plan view observations (any severity of liquefaction) and sectional view observations of severe liquefaction
Hydraulic fracturing	Designate individual penetration tests as locations of marginal liquefaction or no liquefaction based on proximity to observed liquefaction features. Use lowest value of penetration resistance at each test location.	Use highest minimum value of penetration resistance that is common among multiple penetration tests performed in proximity to individual liquefaction features created by hydraulic fracturing.
Lateral spreading	Designate penetration tests within the probable limits of lateral spread as marginal liquefaction. Designate tests outside these limits as no liquefaction. Use highest minimum value of penetration resistance common among multiple tests for each designation.	Use highest minimum value of penetration resistance that is common among penetration tests scattered along the length of the lateral spread (regardless of their proximity to venting features). This length can be hundreds of meters at places subjected to strong earthquake shaking.
Surface oscillations	Same as for hydraulic fracturing. Penetration tests should be performed within a few meters of observed liquefaction feature.	Use highest minimum value of penetration resistance that is commonly present (and typically near the base of the fine-grained cap), and is located within a few tens of meters of the dikes caused by surface oscillations.
Indeterminate mechanism	Same as for hydraulic fracturing	Use lowest value of penetration resistance that is realistically feasible for any of the three candidate mechanisms listed above.

Seismologists commonly estimate the magnitudes and macroseismic epicenter of pre-instrumental earthquakes by comparing intensity (e.g., modified Mercalli intensity) distributions from the pre-instrumental earthquakes to intensity distributions from well-documented recent earthquakes in similar seismotectonic settings (e.g., Hough et al. 2000). The interpretation of seismic intensity data often are complicated by sparse or biased reporting, the effects of local site response (i.e., amplification), and differing regional geology (e.g., Hough et al. 2000), resulting in considerable uncertainty in any one estimate. The approximate isoseismal maps for pre-instrumental events can be compared to those from modern events in terms of isoseismal radii, areas, or other techniques.

It is beyond the scope of this study to quantify the uncertainties associated with estimating the magnitudes and macroseismic epicenters of pre-instrumental earthquakes using intensity methods. However, we recommend accounting for epistemic uncertainties in this step by using a number of estimated pre-instrumental magnitudes and macroseismic epicenters for each earthquake used for developing a regional magnitude bound. The individual estimates can be weighted based on input from seismological experts. Furthermore, we assume that macroseismic epicenters are equivalent to paleoearthquake ‘energy centers<sup>1</sup>,’ as each are defined in a similar manner (Olson et al. 2005b).

Instrumental earthquakes with better defined magnitudes and epicenters should be included in this effort. In these cases, there will often still be some uncertainty in the magnitude estimate, but this should be smaller than the uncertainty associated with pre-instrumental events. However, a potentially greater uncertainty may be related to defining the appropriate site-to-source distance because the location of an energy center (or an intensity center) can differ significantly from an

<sup>1</sup> Centroid of the region of strongest ground shaking based primarily on regional measurements of liquefaction feature size or on back-calculated strength of shaking. Also commonly termed ‘source zone’ or ‘meioseismal zone.’

instrumentally-determined epicenter for larger magnitude earthquakes. For example, data from historical earthquakes in the Wabash Valley region, in the forms of Modified Mercalli Intensities and instrumentally-located epicenters (Rhea and Wheeler 1996), suggest that using liquefaction features to locate the energy center of prehistoric earthquakes generally is accurate within a few tens of kilometers of the instrumental epicenter for earthquakes of moderate size, i.e., less than  $M \sim 6$  (Youd 1977; Obermeier 1998a). At larger magnitudes, this discrepancy can increase greatly (e.g., Gasperini et al. 1999). In these cases, the macroseismic epicenter (i.e., intensity center) should be used rather than the instrumentally-derived epicenter.

Using the weighted macroseismic and/or instrumentally-derived epicenters, a range of site-to-source distances to the most distal liquefaction site can be determined for each earthquake. Again, it is beyond the scope of this study to describe methods for assigning paleoliquefaction features to specific paleoearthquakes. We refer the reader to Munson and Munson (1996) and Obermeier (1996) for a discussion of this issue. By generating random combinations of magnitude and site-to-source distance for each earthquake (we recommend at least 10,000 combinations per earthquake), investigators then can define a region-specific magnitude bound relationship using regression analysis.

### **Developing a framework for paleoliquefaction studies**

We propose using a Bayesian framework that parallels the deterministic approach proposed by Olson et al. (2005a) and Green et al. (2005) to combine uncertainties from disparate sources and maximize the available data and available approaches for paleoliquefaction back-analysis. To be consistent with the Olson et al. (2005a) paleoliquefaction approach, we present the back-analysis considering uncertainties below with respect to the steps proposed by Olson et al. (2005a).

#### ***Step 1. Plan field work***

Plan field work with consideration of regional seismological and geotechnical issues that affect site selection, data interpretation, and details of back-analysis. Olson et al. (2005a) discuss these issues in detail. Planning should be performed with the intent to minimize the uncertainties discussed in this report. However, there are no quantified uncertainties involved in this step.

#### ***Step 2. Perform field work***

Perform field work in light of engineering geologic recommendations of Obermeier et al. (2001, 2005) and data collection techniques suggested by Olson et al. (2005a). A major aspect of the field work should be to define the FDQ for each site that is documented and investigated thoroughly.

#### ***Step 3. Identify provisional paleoearthquake energy center***

Following the field work, use several techniques to define a provisional paleoearthquake energy center. Following the recommendations of Obermeier et al. (2005), investigators can compute individual (x,y) coordinates of the energy center as the centroid of the maximum dike widths at each paleoliquefaction site, the centroid of the sum of the dike widths at each paleoliquefaction

site, and the “linear density” of dikes (i.e., number of dikes per unit length of bank exposure). These coordinate sets can be weighted based on expert opinion. For the three techniques listed above, we recommend using weights of 0.4, 0.4, and 0.2, respectively.

Using the weighted coordinate sets, determine the following parameters: mean and standard deviation of the x-coordinate ( $\mu_x, \sigma_x$ ), mean and standard deviation of the y-coordinate ( $\mu_y, \sigma_y$ ), and the correlation coefficient ( $\rho_{xy}$ ). Using these parameters, generate random points (we used  $10^6$  samples in our analyses) using the corresponding bivariate normal distribution for the provisional energy center and compute source-to-site distances ( $R_{ec}$ ) for each paleoliquefaction site. Because some source-to-site distances do not yield a normal distribution, use the actual samples to define a source-to-site distance distribution for each paleoliquefaction site. This distance distribution will be used in subsequent steps.

***Step 4. Use regional magnitude bound relation to estimate paleomagnitude***

Develop a statistically-based regional magnitude bound as described earlier. For this regional magnitude bound, we recommend weighting individual estimates of earthquake magnitude and maximum source-to-site distance for the most distal liquefaction feature from multiple seismological publications. Using these individual weighted estimates, generate random samples for ( $\mathbf{M}, \mathbf{R}$ ) combinations and regress a relationship to describe the limiting regional magnitude bound.

Using the statistically-based regional magnitude bound and the maximum source-to-site distance distribution ( $R_{ec}$ ) determined in Step 3 (i.e., the distance to the most distal paleoliquefaction site), compute the prior distribution,  $f_M(m)$  for the paleoearthquake magnitude. Use the slope,  $b$ , that corresponds to the region’s magnitude recurrence relationship (e.g., the Gutenberg-Richter relationship) to determine the corresponding minimum and maximum magnitudes ( $\mathbf{M}_{min}$  and  $\mathbf{M}_{max}$ , respectively) that satisfy a truncated exponential distribution such that the area of the probability density function (pdf) is equal to unity.

***Step 5. Perform geotechnical back-analyses at individual paleoliquefaction sites***

Compute the likelihood of liquefaction at individual liquefaction sites, and then combine these likelihoods into a likelihood function for liquefaction occurrence that can be used subsequently in the Bayesian updating framework described in Step 6. The likelihood function is computed as:

$$L(m) = \prod_{site=1}^{site=n} P(C_{site} = D_{site} | m) = \prod_{site=1}^{site=n} \int_0^{\infty} f_C^m(x) \cdot f_D^m(x) \cdot dx \quad [7]$$

where  $C_{site}$  = capacity or liquefaction resistance at a given site and is a function of the normalized penetration resistance (i.e., estimated from Figure 2),  $D_{site}$  = seismic demand computed as discussed below,  $m$  = trial magnitude,  $f_C^m(x)$  = probability density function for capacity at trial magnitude  $m$ ,  $f_D^m(x)$  = probability density function for demand at trial magnitude  $m$ .

The probability density function for seismic demand is computed by combining the estimates of surface ground motion (i.e., bedrock acceleration  $\times$  site response factor) across the magnitude spectrum (from  $\mathbf{M}_{\min}$  to  $\mathbf{M}_{\max}$ ) determined from the attenuation relationships listed in Table 6.

***Step 6. Integrate individual site back-analyses into regional assessment of paleomagnitude***

Combine the likelihood function,  $L(m)$  and the prior distribution,  $f_M(m)$ , using Bayes' theory as follows to compute the posterior distribution for magnitude.

$$f'_M(m) = \kappa \cdot L(m) \cdot f_M(m) \quad [8]$$

where  $\kappa$  is a scaling parameter used to force the posterior probability density function,  $f'_M(m) = 1$ .

The posterior probability density function for magnitude can be used to estimate the mean ( $\mu_M$ ) and standard deviation ( $\sigma_M$ ) for paleoearthquake magnitude.

**TESTBED CASE: VINCENNES EARTHQUAKE**

**Background**

The largest earthquake in the 200-year historical record of the Wabash Valley of Indiana-Illinois (Fig. 1) is M 5.8. However, it is clear from the sizes and abundance of paleoliquefaction features discovered in the region about 10 years ago that much larger Holocene earthquakes had occurred (Obermeier et al., 1993). Most or all the features previously had been attributed to the same large paleoearthquake, estimated to have occurred near Vincennes, Indiana, about 6100 years BP  $\pm$ 200 years (i.e., approximately 5000 calendar years ago; Munson and Munson, 1996) – hereafter referred to as the “Vincennes Earthquake” (e.g., Obermeier et al. 1993; Munson and Munson 1996; Pond 1996; Pond and Martin 1996; Hajic and Wiant 1997; Munson et al. 1997; and Obermeier 1998a), because the largest liquefaction dikes associated with the earthquake are located near Vincennes, Indiana (see Figure 9).

Green et al. (2005) summarize the numerous geologic, engineering geologic, and geotechnical engineering studies that have been performed to identify and date paleoliquefaction features in the region, associate dated paleoliquefaction features with potential paleoearthquakes, and characterize the paleoliquefaction sites for geotechnical back-analysis. They also provide detailed summaries for 12 paleoliquefaction sites used in their back-analysis.

**Paleoliquefaction back-analysis considering uncertainties**

Again, we present the paleoliquefaction back-analysis considering uncertainties below with respect to the steps developed by Olson et al. (2005a). The first two steps, planning and performing the field work, respectively, were performed by others prior to the engineering geologic guidelines and in situ testing approaches proposed by Obermeier et al. (2005) and Olson et al. (2005a) were developed. Therefore, we simply used the data collected by others (for the 12 paleoliquefaction sites examined by Green et al. (2005) to the extent possible. These data

along with our estimates of standard deviations, COV, and boundary values are summarized in Table 8.

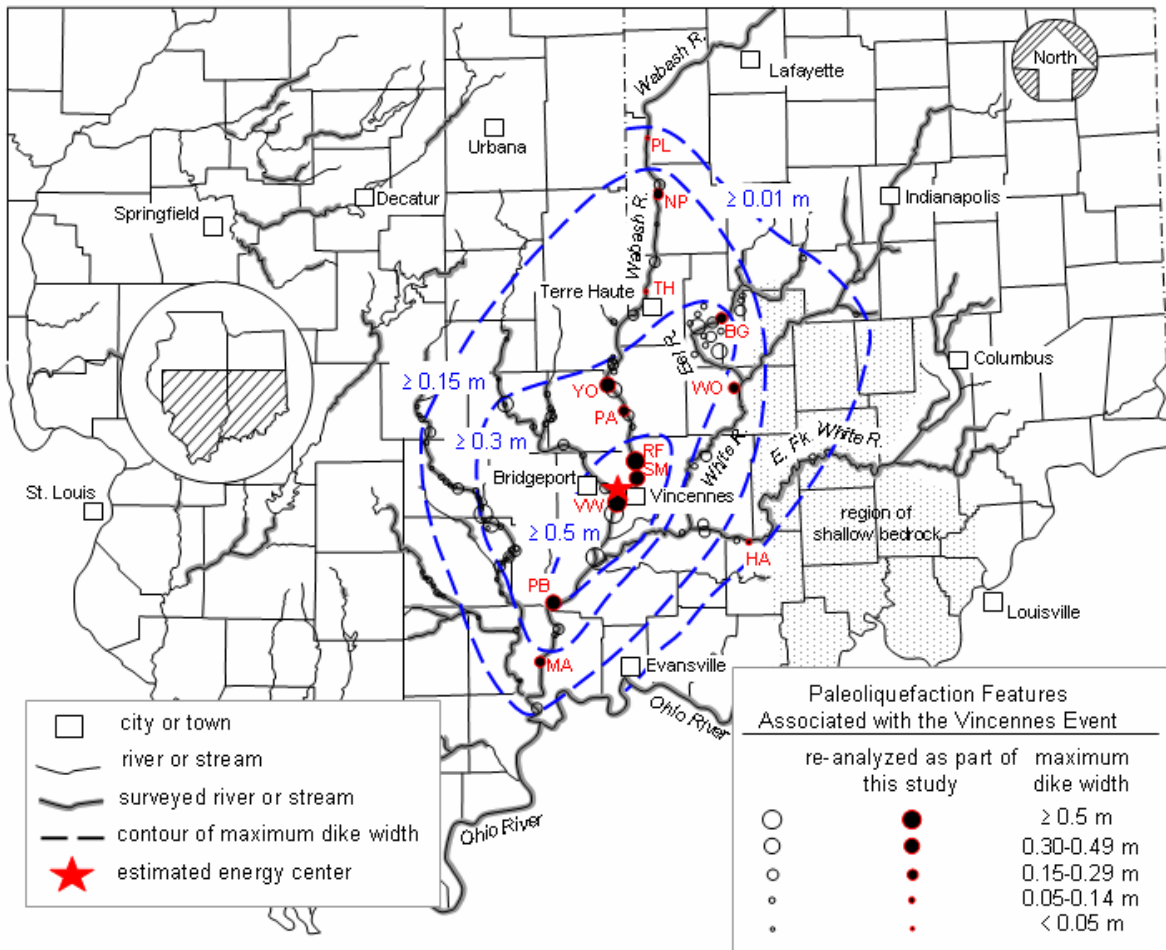


**Figure 9. Map of paleoliquefaction sites in the Wabash Valley (adapted from Munson and Munson, 1996; Hajic and Wiant, 1997; Obermeier, 1998a). Energy center shown in the figure was estimated deterministically.**

### ***Step 3. Identify provisional paleoearthquake energy center***

Using measured dike widths (Munson and Munson 1996; Hajic and Wiant 1997) for dikes associated with the Vincennes earthquake, we computed (x,y) coordinates for the provisional energy center using the centroid of the maximum dike widths, which Obermeier et al. (2005) consider to be the most reliable. This approach provided a “best estimate” as well as upper and lower bound positions for the provisional energy center depending on how the dike widths were interpreted. We weighted these (x,y) coordinates along with the deterministically determined energy center (Obermeier and Pond 1999) as follows.

Figure 10 provides the distributions of source-to-site distance computed during this study.

**Table 8. Input data used for back-analysis of Vincennes paleoearthquake**

Site	Liq.		Z <sub>liq</sub> (m)				Z <sub>gwt</sub> (m)				Unit weight		N-value		FC (%)			
			FDQ	severity	μ	σ	l/b	u/b	μ	σ	l/b	u/b	μ	COV	μ	COV	COV	
	(kN/m <sup>3</sup> )	(%)											(%)	(%)		μ	(%)	l/b
VW	H	1	6.1	0.7	2.0	9.0	1.5	0.3	0	Z <sub>liq</sub>	18.5	5	27	25	4	15	0	20
SM	H	3	2.4	0.4	1.0	10.0	0.23	0.2	0	Z <sub>liq</sub>	18.5	5	7	25	4	15	0	20
RF	H	3	3.2	0.7	2.0	12.0	1.2	0.25	0	Z <sub>liq</sub>	18.5	5	19	25	4	15	0	20
PA	H	2	2.4	0.7	1.5	9.0	2.3	0.3	0	Z <sub>liq</sub>	18.5	5	12	25	4	15	0	20
PB	H	3	6.1	1.0	2.0	10.0	2.3	0.3	0	Z <sub>liq</sub>	18.5	5	20	25	4	15	0	20
YO	L	3	4.8	0.7	3.5	9.0	3.1	0.55	0	Z <sub>liq</sub>	18.5	15	10	45	4	35	0	20
MA	H	2	2.3	0.4	1.5	4.5	1.2	0.3	0	Z <sub>liq</sub>	18.5	5	9.5	25	10	15	0	35
WO	H	2	2.7	0.3	1.5	10.0	1.5	0.2	0	Z <sub>liq</sub>	18.5	5	7	25	15	15	0	35
TH	L	2	5.2	0.7	3.5	8.0	0.76	0.7	0	Z <sub>liq</sub>	18.5	15	14.5	25	4	35	0	20
BG	L	1	5.3	0.4	4.0	8.0	2.3	0.5	0	Z <sub>liq</sub>	18.5	15	3.5	45	4	35	0	20
NP	I	2	3.2	0.5	2.0	6.5	2.0	0.3	0	Z <sub>liq</sub>	18.5	10	6	35	4	25	0	20
PL	L	2	5.5	0.8	4.0	8.0	0.75	0.75	0	Z <sub>liq</sub>	18.5	15	8	45	4	35	0	20

Notes: (1) μ = mean; σ = standard deviation; l/b = lower bound; u/b = upper bound; COV = coefficient of variation  
 (2) FDQ = field data quality; H = high; I = intermediate; L = low  
 (3) Liquefaction severity: 0 = no liquefaction; 1 = marginal; 2 = moderate; 3 = severe liquefaction  
 (4) Z<sub>liq</sub> = depth to likely zone of liquefaction at time of earthquake (ATE); Z<sub>gwt</sub> = depth to ground water table ATE  
 (5) N-value = measured SPT blow count (blows/0.3m)  
 (6) FC = measured fines content (%)

**Table 9. Weights provided to provisional energy center estimates for Vincennes Earthquake**

Approach	Reference	Weight
Centroid of maximum dike widths (best estimate)	This study	0.3
Centroid of maximum dike widths (upper bound)	This study	0.1
Centroid of maximum dike widths (lower bound)	This study	0.1
Deterministic energy center	Obermeier (1998a)	0.5

**Step 4. Use regional magnitude bound relation to estimate paleomagnitude**

Using the approach described above and the CEUS earthquake data provided by Olson et al. (2005b), we used a mathematical function to define a regional magnitude bound for the CEUS. Figure 11 presents the analysis and regressed magnitude bound. A 2<sup>nd</sup> order polynomial ( $M = a_1 \log_{10}(R)^{a_2} + a_3$ ) provided the best fit to the CEUS earthquake data, and as illustrated in the figure, the regressed mathematical form is almost identical to the deterministic bound proposed by Olson et al. (2005b) and matches Ambraseys (1988) at distances greater than 20 km.

Using the maximum source-to-site distance distribution above and the statistically-based magnitude bound relationship presented in Figure 11, we developed a truncated exponential distribution for magnitude. We used  $b = 0.96$  based on recommendations of Frankel et al. (2002). Figure 12 presents the truncated exponential distribution.

**Step 5. Perform geotechnical back-analyses at individual paleoliquefaction sites**

Figure 13 presents the probability density function for capacity and the probability density function for demand at site PA. The probability density functions for the other sites were similar. Combining the likelihood for liquefaction at each site, we developed an aggregate likelihood function from the liquefaction evidence, as shown in Figure 14.

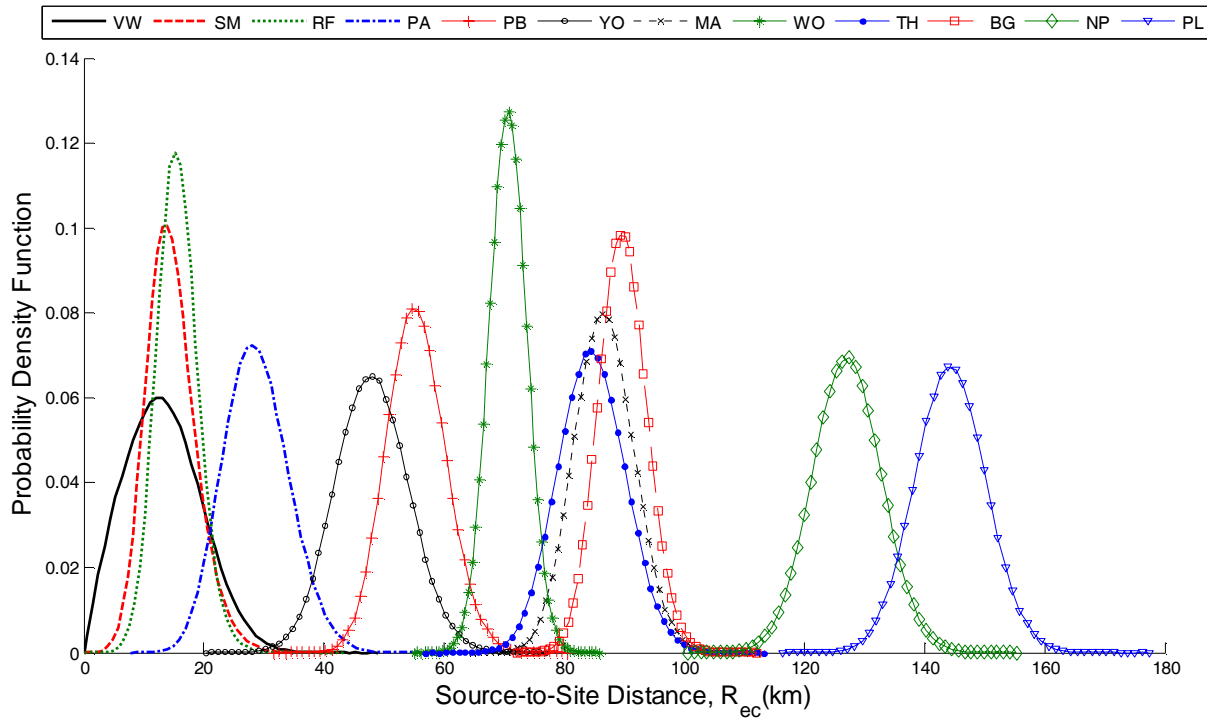


Figure 10. Probability density functions of the source-to-site distances for the 12 paleoliquefaction sites examined in this study

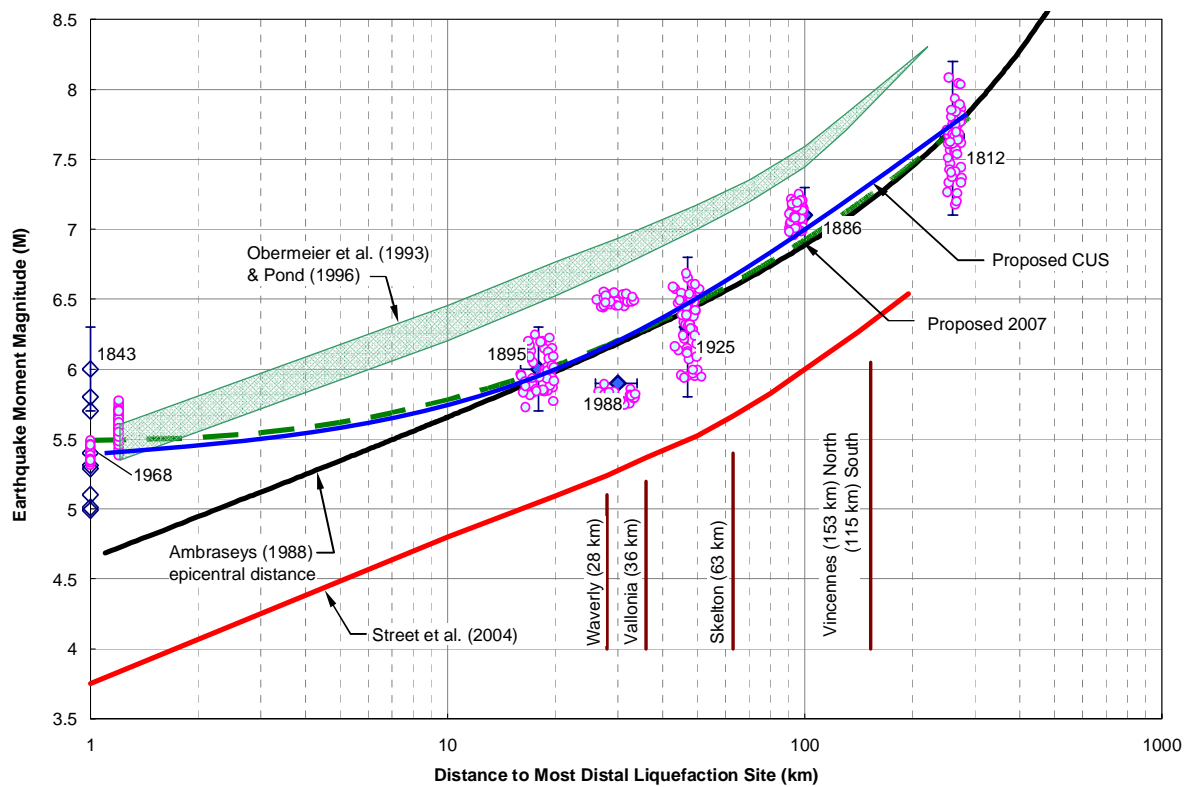


Figure 11. Statistically-based magnitude bound for CEUS (adapted from Olson et al. 2005b). The small data points are a fraction of the 10,000 random sampling points generated for each earthquake. For simplicity, we used the aggregate ( $\mu, \sigma$ ) combinations for  $M$  and  $R$  for each historical earthquake in this analysis.

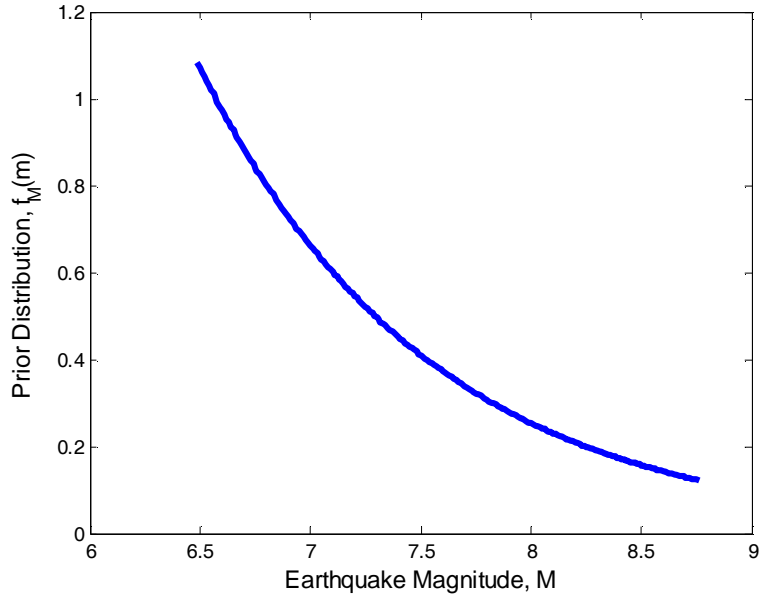


Figure 12. Prior distribution of Vincennes paleoearthquake magnitude based on regional magnitude bound and most distal liquefaction site.

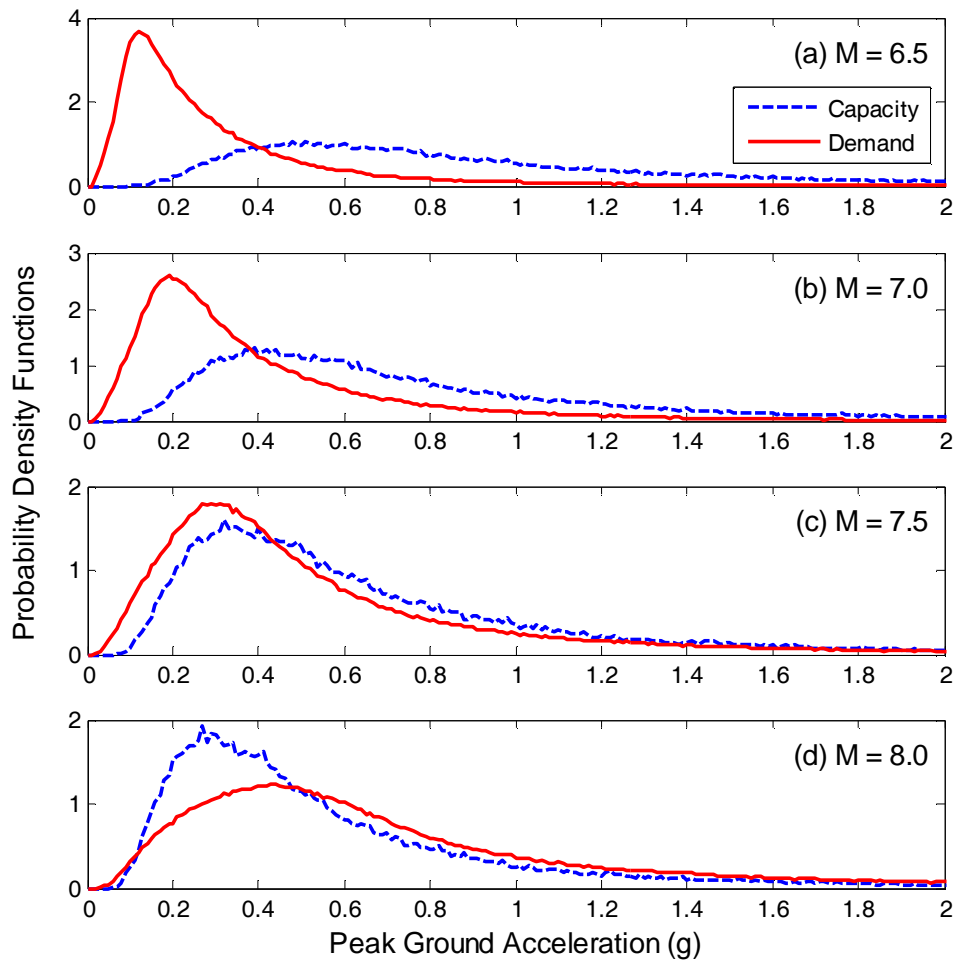


Figure 13. Probability density functions of capacity and demand for Site PA for four trial magnitudes

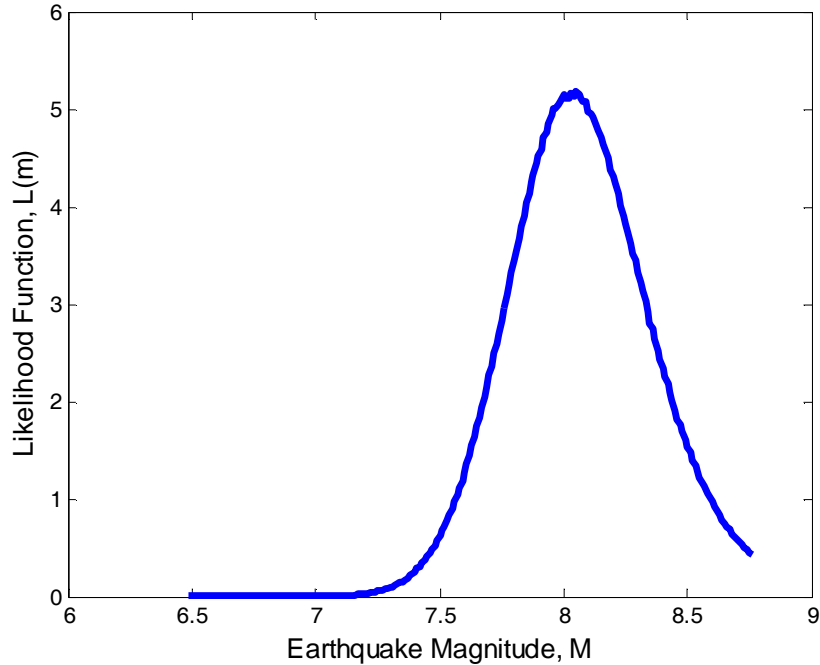


Figure 14. Likelihood function for magnitude for the Vincennes paleoearthquake

**Step 6. Integrate individual site back-analyses into regional assessment of paleomagnitude**

As discussed above, the aggregate likelihood function is used to update the prior distribution for paleomagnitude estimated in Step 4. Figure 15 presents the resulting posterior distribution for paleoearthquake magnitude. Based on these analyses, we preliminarily estimate the magnitude for the Vincennes earthquake as  $7.99 \pm 0.27$ .

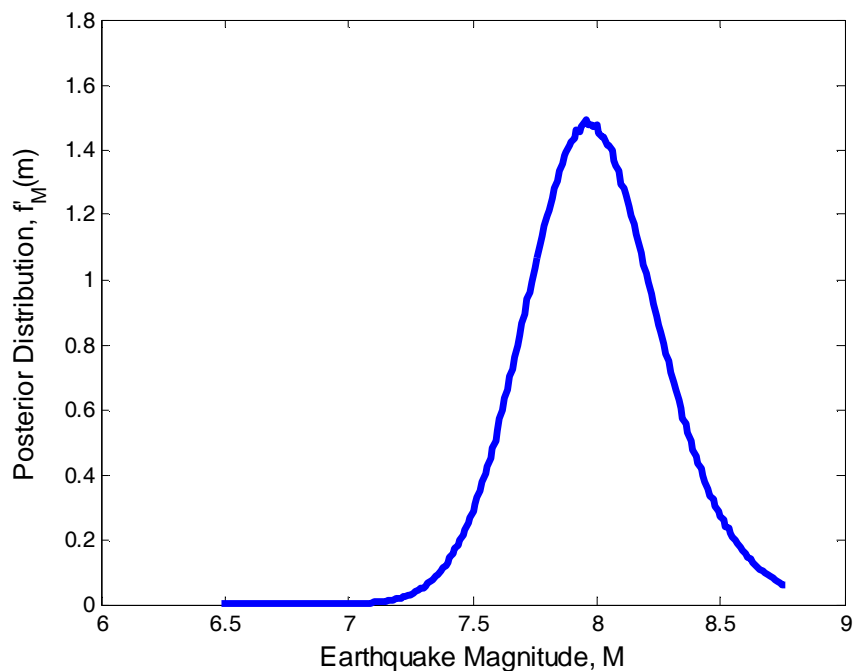


Figure 15. Posterior distribution for paleoearthquake magnitude for the Vincennes earthquake

## Comparison with other paleoliquefaction studies

The preliminary estimate for the magnitude of the Vincennes earthquake of  $7.99 \pm 0.27$  is somewhat larger than the estimates of 7.8 from Pond (1996); 7.7 – 7.8 from Obermeier and Pond (1999); 7.5 from Green et al. (2005); and 7.3 from Olson et al. (2005b). However, this approach explicitly accounts for many of the uncertainties associated with a typical paleoliquefaction analysis, and provides a slightly larger, but still reasonable, estimate of paleomagnitude.

## CONCLUSIONS AND FUTURE WORK

Paleoliquefaction studies are important aspects of paleoseismic studies in regions where historical records are too short to assess earthquake recurrence and where active faults do not reach the ground surface (where they can be directly studied). However, until now, paleoliquefaction studies have been entirely deterministic, without direct consideration of the numerous uncertainties involved in the back-analysis.

This study represents an initial attempt to identify and quantify the numerous uncertainties involved in a paleoliquefaction back-analysis using the procedure proposed by Olson et al. (2005a). These uncertainties include those related to (Olson et al. 2007): (1) liquefaction susceptibility (specifically aging and density change; liquefaction severity; fines content adjustment; and overburden stress correction); (2) field observations, ground failure mechanism, and field setting [which are assessed using a *field data quality* (FDQ) factor (Green et al. 2005) for specific parameters such as unit weight and fines content]; (3) seismicity and seismic demand (i.e., attenuation relationships; magnitude scaling factors (MSF); depth reduction factor,  $r_d$ ; and local site response; and (4) validity of in situ testing techniques, including selecting a representative penetration resistance (again assessed using FDQ). In the magnitude bound method, additional uncertainties occur due to the need to regionally calibrate the method using historic earthquakes in the same tectonic setting.

We propose a combination of simplified and rigorous statistical and probabilistic methods to treat these uncertainties. Aleatoric uncertainties (such as fines content) are treated by considering these parameters to be normally- or lognormally-distributed variables. Epistemic uncertainties (such as fines content adjustment) are treated by using a logic tree approach with weighted branches. These uncertainties are combined in a Bayesian updating framework that uses the magnitude bound method to estimate a prior distribution, aggregate observations from individual paleoliquefaction site back-analyses to compute a likelihood function, and the product of the prior distribution and the likelihood function to compute a posterior distribution for the paleoearthquake magnitude.

The proposed procedure was preliminarily applied to the Vincennes earthquake (circa 6100 yr BP). The back-analysis considering uncertainties yielded a  $M \sim 7.99 \pm 0.27$ . This estimate is somewhat larger than deterministic estimates of 7.3 to 7.8 made by other investigators, but this estimate is the first to explicitly consider the uncertainties in the paleoliquefaction back-analysis. As such, it provides guidance regarding the reliability of the magnitude estimates.

In the future we intend to investigate the effect of using different  $b$ -values on the prior distribution for paleoearthquake magnitude. For example, Cramer (2001) recommends a  $b$ -value of 0.8 for the NMSZ. Using a lower  $b$ -value could influence the prior (and therefore the posterior) distribution significantly. We also intend to investigate other tools (such as the liquefaction potential index proposed by Iwasaki et al. 1978) to account for liquefaction severity, particularly those that would let us utilize sites of no liquefaction. (“No liquefaction” sites can not be used with the  $FS_{liq}$  approach proposed here.)

## ACKNOWLEDGEMENTS

The authors would like to thank Dr. Thomas Holzer and Dr. Michael Bennett (USGS) for providing us with digital CPT soundings performed following the 1989 Loma Prieta earthquake, Prof. John Berrill (University of Christchurch, New Zealand) for providing us with digital CPT soundings performed following the 1987 Edgecumbe earthquake, Prof. Ron Andrus (Clemson University) for providing us with digital CPT soundings performed following the 1986 Borah Peaks earthquake, and Prof. Robert Moss for providing us with several University of California at Berkeley reports. The authors also are indebted to Dr. Steve Obermeier for providing us with several reports related to the Vincennes earthquake and to Dr. Obermeier and Prof. Russell Green for discussing with us many of the concepts presented in this study.

## REFERENCES

- Algermissen, S.T., Perkins, D.M., Thenhaus, P.C., Hanson, S.L., and Bender, B.L. (1982). Probabilistic estimates of maximum acceleration and velocity in rock in the contiguous United States. *U.S. Geological Survey Open-File Report 82-1033*, Washington, DC, 99 pp.
- Ambraseys, N.N. (1988). Engineering seismology. *Earthquake Engineering and Structural Dynamics*, 17, 1-105.
- Amick, D., Gelinis, R., Maurath, G., Cannon, R., Moore, D., Billington, E., and Kempainen, H. (1990). Paleoliquefaction features along the Atlantic seaboard. *NUREG/CR-5613*, Washington, DC, Nuclear Regulatory Commission.
- Andrus, R.D. and Stokoe II, K.H. (1997). Liquefaction resistance based on shear wave velocity. *Proc., NCEER Workshop on Evaluation of Liquefaction Resistance of Soils*, in: T.L. Youd and I.M. Idriss, I.M., (eds.), Technical Report NCEER-97-0022, State Univ. of New York at Buffalo, NY, 89-128.
- Arango, I. (1996). Magnitude scaling factors for soil liquefaction evaluations. *ASCE Journal of Geotechnical Engineering*, 122(11), 929-936.
- Arulanandan, K., Yogachandran, C., Meegoda, N.J., Ying, L., and Zhauji, S. (1986). Comparison of the SPT, CPT, SV and electrical methods of evaluating earthquake induced liquefaction

susceptibility in Ying Kou City during the Haicheng earthquake. *Proc., Use of In Situ Tests in Geotechnical Engineering*, Geotechnical Specialty Publication No. 6, ASCE, New York, NY, 389-415.

Atkinson, G.M. and Boore, D.M. (1995). New ground motions relations for eastern North America. *Bulletin of the Seismological Society of America*, 85, 17-30.

Baecher, G.B. and Christian, J.T. (2003). *Reliability and Statistics in Geotechnical Engineering*, John Wiley and Sons Ltd., 605 p.

Baziar, M.H., Dobry, R., and Elgamal, A-W.M. (1992). Engineering evaluation of permanent ground deformations due to seismically-induced liquefaction. *Technical Report NCEER-92-0007*, National Center for Earthquake Engineering Research, State University of New York at Buffalo, Buffalo, NY.

Bennett, M.J. (1989). Liquefaction analysis of the 1971 ground failure at the San Fernando Valley Juvenile Hall, California. *Bulletin of the Association of Engineering Geologists*, 26(2), 209-226.

Bennett, M.J. (1990). Ground deformation and liquefaction of soil in the Marina district. *Effects of the Loma Prieta Earthquake on the Marina District, San Francisco, California*, Open-file Report 90-253, Dept. of the Interior, U.S. Geological Survey, Denver, CO, 44-79.

Bennett, M.J. and Tinsley, J.C., III. (1995). Geotechnical data from surface and subsurface samples outside of and within liquefaction related ground failures caused by the October 17, 1989, Loma Prieta earthquake, Santa Cruz and Monterey Counties, California. *U.S. Geological Survey Open-File Rep. 95-663*, U.S. Geological Survey, Menlo Park, CA.

Bennett, M.J., Youd, T.L., Harp, E.L, and Wieczorek, G.F. (1981). Subsurface investigation of liquefaction, Imperial Valley earthquake, California, October 15, 1979. *U.S. Geological Survey Open-file Report 81-502*, 87 p.

Bennett, M.J., McLaughlin, P.V., Sarmiento, J.S., and Youd, T.L. (1984). Geotechnical investigation of liquefaction sites, Imperial Valley, California. *U.S. Geological Survey Open-file Report 84-252*, 108 p.

Bennett, M.J., Ponti, D.J., Tinsley, J.C. III, Holzer, T.L., and Conaway, C.H. (1998). Subsurface geotechnical investigations near sites of ground deformation caused by the January 17, 1994, Northridge, California, earthquake. *U.S. Geological Survey Open-file Report 98-373*, 148 p.

Boulanger, R.W., Idriss, I.M., and Mejia, L.H. (1995). Investigation and evaluation of liquefaction related ground displacements at Moss Landing during the 1989 Loma Prieta earthquake. *Report No. UCD/CGM-95/02*, Center for Geotechnical Modeling, Department of Civil & Environmental Engineering, University of California at Davis.

Boulanger, R.W., Mejia, L.H., and Idriss, I.M. (1997). Liquefaction at Moss Landing during Loma Prieta earthquake. *ASCE Journal of Geotechnical and Geoenvironmental Engineering*, 123(5), 453-467.

Boulanger, R.W., Meyers, M.W., Mejia, L.H., and Idriss, I.M. (1998). Behavior of a fine-grained soil during Loma Prieta earthquake. *Canadian Geotechnical Journal*, 35, 146-158.

Bray, J.D. (2000). Documenting incidents of ground failure resulting from the August 17, 1999 Kocaeli, Turkey earthquake. <<http://peer.berkeley.edu/publications/turkey/adapazari/index.html>>

Bray, J.D., Sancio, R.B., Youd, T.L., Durgunoglu, H.T., Onalp, A., Cetin, K.O., Seed, R.B., Stewart, J.P., Christensen, C., Baturay, M.B., Karadayilar T., and Emrem, C. (2003). Documenting incidents of ground failure resulting from the August 17, 1999 Kocaeli, Turkey earthquake: data report characterizing subsurface conditions. *Geoengineering Research Report No. UCB/GE-03/02*, University of California at Berkeley, Berkeley, CA, 588 p.

Bray, J.D., Stewart, J.P., (coordinators and principal contributors), Baturay, M.B., Durgunoglu, T., Onalp, A., Sancio, R.B., Ural, D. (principal contributors). (2000). Damage patterns and foundation performance in Adapazari. Chapter 8 of the Kocaeli Turkey earthquake of August 17, 1999 reconnaissance report. *Earthquake Spectra*, Earthquake Engineering Research Institute, 16 (Suppl A), 163-189.

Campbell, K.W. (2003). Prediction of strong ground motion using the hybrid empirical method and its use in the development of ground-motion (attenuation) relations in eastern North America. *Bulletin of the Seismological Society of America*, 93(3), 1012-1033.

Campbell, K.W. (2004). *Erratum* to “Prediction of strong ground motion using the hybrid empirical method and its use in the development of ground-motion (attenuation) relations in eastern North America.” *Bulletin of the Seismological Society of America*, 86, 2418.

Cetin, K.O., Seed, R.B., Moss, R.E.S., Der Kiureghian, A., Tokimatsu, K. Harder, L.F. Jr., and Kayen, R.E. (2000). Field case histories for SPT-based in situ liquefaction potential evaluation. *Geotechnical Engineering Research Report No. UCB/GT-2000/09*.

Cetin, K.O., Youd, T.L., Seed, R.B., Bray, J.D., Sancio, R., Lettis, W., Yilmaz, M.T., and Durgunoglu, H.T. (2002). Liquefaction-induced ground deformations at Hotel Sapanca during Kocaeli (Izmit), Turkey earthquake. *Soil Dynamics and Earthquake Engineering*, 22, 1083-1092.

Cetin, K.O., Seed, R.B., Kiureghian, A.D., Tokimatsu, K., Harder, L.F., Jr., Kayen, R.E., and Moss, R.E.S. (2004a). Standard penetration test-based probabilistic and deterministic assessment of seismic soil liquefaction potential. *ASCE Journal of Geotechnical and Geoenvironmental Engineering*, 130(12), 1314–1340.

Cetin, K.O., Youd, T.L., Seed, R.B., Stewart, J.P., Durgunoglu, H.T., Lettis, W.R., and Yilmaz, M.T. (2004b). Liquefaction-induced lateral spreading at Izmit Bay during the Kocaeli (Izmit)-

Turkey earthquake. *ASCE Journal of Geotechnical and Geoenvironmental Engineering*, 130(12), 1300-1313.

Charlie, W.A., Doehring, D.O., Brislawn, J.P., and Hassen, H. (1998). Direct measurement of liquefaction potential in soils of Monterey County, California. *U.S. Geological Survey Professional Paper 1551-B*, U.S. Department of the Interior, 181-222.

Christensen, S.A. (1995). Liquefaction of cohesionless soils in the March 2, 1987 Edgecumbe earthquake, Bay of Plenty, New Zealand, and other Earthquakes. *Masters of Engineering Thesis*, Dept. of Civil Engineering, University of Canterbury, Christchurch, New Zealand.

Christian, J.T. and Swiger, W.F. (1975). Statistics of liquefaction and SPT results. *ASCE Journal of the Geotechnical Engineering Division*, 101(11), 1135-1150.

Chu, D.B., Stewart, J.P., Lee, S., Tsai, J.S., Lin, P.S., Chu, B.L., Seed, R.B., Hsu, S.C., Yu, M.S., and Wang, M.C.H. (2004). Documentation of soil conditions at liquefaction and non-liquefaction sites from 1999 Chi-Chi (Taiwan) earthquake. *Soil Dynamics and Earthquake Engineering*, 24 (9-10), 647-657.

Chu, D.B., Stewart, J.P., Youd, T.L., and Chu, B.L. (2006). Liquefaction-induced lateral spreading in near-fault regions during the 1999 Chi-Chi, Taiwan earthquake. *ASCE Journal of Geotechnical and Geoenvironmental Engineering*, 132(12), 1549-1565.

Cornell, C.A. (1968). Engineering seismic risk analysis. *Bulletin of the Seismological Society of America*, 58, 1583-1606.

Cramer, C.H. (2001). A seismic hazard uncertainty analysis for the New Madrid seismic zone. *Engineering Geology*, 62, 251-266.

Dai, S.-H. and Wang, M.-O. (1992). *Reliability analysis in engineering applications*. Van Nostrand Reinhold, New York.

Dobry, R., Ladd, R.S., Yokel, F.Y., Chung, R.M., and Powell, D. (1982). Prediction of pore water pressure buildup and liquefaction of sands during earthquakes by the cyclic strain method. *NBS Building Science Series*, vol. 138, U.S. Dept. of Commerce, 152 p.

Duncan, J.M. (2000). Factors of safety and reliability in geotechnical engineering. *ASCE Journal of Geotechnical and Geoenvironmental Engineering*, 126(4), 307-316.

Farrar, J.A. (1990). Study of in situ testing for evaluation of liquefaction resistance. *Report No. R-90-06*, U.S. Department of the Interior, Bureau of Reclamation, 133 p.

Finn, W.D.L. (2002). State of the art for the evaluation of seismic liquefaction potential. *Computers and Geotechnics*, 29, 329-341.

Frankel, A., Mueller, C., Barnhard, T., Perkins, D., Leyendecker, E.V., Dickman, N., Hanson, S., and Hopper, M. (1996). National seismic-hazard maps: documentation. *U.S. Geological Survey Open-File Report 96-532*, U.S. Department of the Interior.

Frankel, A.D., Petersen, M.D., Mueller, C.S., Haller, K.M., Wheeler, R.L., Leyendecker, E.V., Wesson, R.L., Harmsen, S.C., Cramer, C.H., Perkins, D.M., and Rukstales, K.S. (2002). Documentation for the 2002 update of the National Seismic Hazard Maps. *U.S. Geological Survey Open-file Report 02-420*, U.S. Department of the Interior, 33 p.

Gasperini, P., Bernardini, F., Valensise, G., Boschi, E. (1999). Defining seismogenic sources from historical earthquake felt reports. *Bulletin of the Seismological Society of America*, 89, 94-110.

Gilstrap, S.D., and Youd, T.L. (1998). CPT based liquefaction resistance analyses using case histories. *Technical Report CEG-90-01*, Dept. of Civ. and Env. Eng., Brigham Young University, Provo, Utah.

Green, R.A. (2001). Energy-based evaluation and remediation of liquefiable soils. *PhD Thesis*, Virginia Polytechnic Institute and State University, Blacksburg, VA, 397 pp.

Green, R.A., and Mitchell, J.K. (2003). A closer look at Arias intensity based liquefaction evaluation procedures. *Proc., 7th Pacific Conference on Earthquake Engineering*, Univ. of Canterbury, Christchurch, New Zealand, Feb. 13-15, Paper No. 94. 9 p.

Green, R.A., Obermeier, S.F., and Olson, S.M. (2005). Engineering geologic and geotechnical analysis of paleoseismic shaking using liquefaction effects: field examples. *Engineering Geology*, 76, 263-293.

Green, R.A., Olson, S.M., and Polito, C. (2006). A comparative study of the influence of fines on the liquefaction susceptibility of sands: field versus laboratory. *Proc. 8th National Earthquake Engineering Conf.*, San Francisco, CA, April.

Hajic, E.R. and Wiant, M.D. (1997). Dating of prehistoric earthquake liquefaction in southeastern and central Illinois. *Final Report to the U.S. Geological Survey*, 57 p.

Haldar, A., and Tang, W.H. (1979). Probabilistic evaluation of liquefaction potential. *ASCE Journal of Geotechnical Engineering*, 105(2), 145-163.

Hamada, M. Isoyama, R., and Wakamatsu, K. (1996). Liquefaction-induced ground displacement and its related damage to lifeline facilities. *Special Issue of Soils and Foundations on the Geotechnical Aspects of the January 17, 1995, Hyogoken-Nambu Earthquake*, 81-97.

Harder, L.F., Jr. and Boulanger, R.W. (1997). Application of  $K_{\sigma}$  and  $K_{\alpha}$  correction factors. *Proc., NCEER Workshop on Evaluation of Liquefaction Resistance of Soils*, National Center for Earthquake Engineering Research, State Univ. of New York at Buffalo, 167-190.

- Harr, M.E. (1987). *Reliability-based Design in Civil Engineering*. McGraw-Hill Book Company.
- Holzer, T.L., Bennett, M.J., Ponti, D.J., and Tinsley, J.C.I. (1999). Liquefaction and soil failure during 1994 Northridge earthquake. *ASCE Journal of Geotechnical Engineering*, 125(6), 438-452.
- Holzer, T.L., Tinsley, J.C.I., Bennett, M.J., and Mueller, C.S. (1994). Observed and predicted ground deformation – Miller Farm lateral spread, Watsonville, California. *Proc. 5<sup>th</sup> U.S.-Japan Workshop on Earthquake Resistant Design of Lifeline Facilities and Countermeasures for Soil Liquefaction*, Technical Report NCEER-94-0026, 79-99.
- Holzer, T.L., Youd, T.L., and Hanks, T.C. (1989). Dynamics of liquefaction during the 1987 Superstition Hills, California, earthquake. *Science*, 244, 56-59.
- Hough, S.E., Armbruster, J.G., Seeber, I., and Hough, J.F. (2000). On the modified Mercalli intensities and magnitudes of the 1811-1812 New Madrid earthquakes. *Journal of Geophysical Research*, 105, 23,839-23,864.
- Hwang, J.-H. and Yang, C.-W. (2001). Verification of critical cyclic strength curve by Taiwan Chi-Chi earthquake data. *Soil Dynamics and Earthquake Engineering*, 21, 237-257.
- Idriss, I.M. (1990). Response of soft soil sites during earthquakes, *Proc. H. Bolton Seed Memorial Symposium*, J.M. Duncan, ed., Univ. of California, Berkeley, 2, 273-289.
- Idriss I.M. (1999). An update to the Seed-Idriss simplified procedure for evaluating liquefaction potential. *Proc., TRB Workshop on New Approaches to Liquefaction*, January, Publication No. FHWA-RD-99-165, Federal Highway Administration.
- Idriss, I.M. and Boulanger, R.W. (2006). Semi-empirical procedures for evaluating liquefaction potential during earthquakes. *Soil Dynamics and Earthquake Engineering*, 26, 115-130.
- Ishihara, K. and Koga, Y. (1981). Case studies of liquefaction in the 1964 Niigata earthquake. *Soils and Foundations*, 21(3), 35-52.
- Iwasaki, T., Tatsuoka, F., Tokida, K.-I., and Yasuda, S. (1978). A practical method for assessing soil liquefaction potential based on case studies at various sites in Japan. *Proc., 2<sup>nd</sup> Intl. Conf. on Microzonation*, San Francisco, 885-896.
- Jones, A.L., Kramer, S.L., and Arduino, P. (2002). Estimation of uncertainty in geotechnical properties for performance-based earthquake engineering. *PEER Report 2002/16*, Pacific Earthquake Engineering Research Center, University of California at Berkeley, 100 p.
- Juang, C.H. (2002). Soil liquefaction in the 1999 Chi-Chi, Taiwan, earthquake. <http://www.ces.clemson.edu/chichi/>

- Juang, C.H., Chen, C.J., Rosowsky, D.V., and Tang, W.H. (2000b). CPT-based liquefaction analysis. Part 2: Reliability for design. *Geotechnique*, 50(5), 593-599.
- Juang, C.H., Fang, S.Y., and Khor, E.H. (2006). First-order reliability method for probabilistic liquefaction triggering analysis using CPT. *ASCE Journal of Geotechnical and Geoenvironmental Engineering*, 132(3), 337-350.
- Juang, C.H., Rosowsky, D.V., and Tang, W.H. (1999). Reliability-based method for assessing liquefaction potential of soils. *ASCE Journal of Geotechnical and Geoenvironmental Engineering*, 125(8), 684-689.
- Juang, C.H., Yuan, H., Lee, D.-H., Ku, C.-S. (2002). Assessing CPT-based methods for liquefaction evaluation with emphasis on the cases from the Chi-Chi, Taiwan, earthquake. *Soil Dynamics and Earthquake Engineering*, 22, 241-258.
- Juang, C.H., Yuan, H., Li, D.K., Yang, S.H., and Christopher, R.A. (2005). Estimating severity of liquefaction-induced damage near foundation. *Soil Dynamics and Earthquake Engineering*, 25, 403-411.
- Kanatani, M., Kiku, C., Yasuda, S., Yoshida, C., Ishihara, K., Kokusho, T., Miura, M., Goto, Y. and Morimoto, I. (2003). Damages on waterfront ground during the 1999 Kocaeli earthquake in Turkey. *Soils and Foundations*, 43(5), 29-40.
- Kayen, R.E. and Mitchell, J.K. (1997). Assessment of liquefaction potential during earthquakes by Arias intensity. *ASCE Journal of Geotechnical and Geoenvironmental Engineering*, 123(12), 1162-1174.
- Kayen, R.E., Mitchell, J.K., Seed, R.B., and Nishio, S. (1998). Soil liquefaction in the East Bay D during the earthquake. *U.S. Geological Survey Professional Paper 1551-B*, U.S. Department of the Interior, 61-86.
- Ku, C.-S., Lee, D.-H., Wu, J.-H. (2004). Evaluation of soil liquefaction in the Chi-Chi, Taiwan earthquake using CPT. *Soil Dynamics and Earthquake Engineering*, 24, 659-673.
- Kulhawy, F.H. (1992). On the evaluation of soil properties. *ASCE Geotechnical Special Publication No. 31*, 95-115.
- Kulhawy, F.H. and Trautmann, C.H. (1996). Estimation of in-situ test uncertainty. *Proc., Uncertainty in the Geologic Environment*, Vol. 1, Madison, WI, 269-286.
- Kulkarni, R.B., Sudigh, K., and Idriss, I.M. (1979). Probabilistic evaluation of seismic exposure. *Proc., 7<sup>th</sup> World Conference on Earthquake Engineering*, San Francisco, CA, 90-98.
- Kulkarni, R.B., Youngs, R.R., and Coppersmith, K.J. (1984). Assessment of confidence intervals for results of seismic hazard analysis. *Proc., 8<sup>th</sup> World Conference on Earthquake Engineering*, San Francisco, CA, Vol. 1, 263-270.

Lacasse, S. and Nadim, F. (1996). Uncertainties in characterising soil properties. *Uncertainty in the Geologic Environment: from Theory to Practice*, Proceedings of Uncertainty '96, ASCE Geotechnical Special Publication No. 58, Vol. 1, 49-75.

Liao, S.S.C., Veneziano, D., and Whitman, R.V. (1988). Regression models for evaluating liquefaction probability. *ASCE Journal of Geotechnical Engineering*, 114(4), 389-411.

McCalpin, J.P., editor. (1996). *Paleoseismology*. Academic Press, San Diego.

McGuire, R.K. (2004). Seismic Hazard and Risk Analysis. *Earthquake Engineering Research Institute Second Monograph Series*, MNO-10, Oakland, CA.

Mejia, L.H. (1998). Liquefaction at Moss Landing. *U.S. Geological Survey Professional Paper 1551-B*, U.S. Department of the Interior, 129-150.

Mesri, G., Feng, T.W., and Benak, J.M. (1990). Postdensification penetration resistance of clean sands. *ASCE Journal of Geotechnical Engineering*, 116(7), 1095-1115.

Metzger, A.G. (1996). "New" historical earthquakes in the New Madrid seismic zone. *Seismological Research Letters*, 67(2), 47.

Mitchell, J.K., Lodge, A.L., Coutinho, R.Q., Kayen, R.E., Seed, R.B., Nishio, S., Stokoe, K.H., II. (1994). Insitu test results from four Loma Prieta earthquake liquefaction sites: SPT, CPT, DMT, and shear wave velocity. *Earthquake Engineering Research Center Report No. UCB/EERC-94/04*, University of California at Berkeley, Berkeley, CA, 179 p.

Moss, R.E.S. (2003). CPT-based probabilistic assessment of seismic soil liquefaction initiation. *PhD Thesis*, University of California at Berkeley, Berkeley, CA.

Moss, R.E.S., Seed, R.B., Kayen, R.E., Stewart, J.P., Kiureghian, A.D., and Cetin, K.O. (2006). CPT-based probabilistic and deterministic assessment of in situ seismic soil liquefaction potential. *ASCE Journal of Geotechnical and Geoenvironmental Engineering*, 132(8), 1032-1051.

Munson, P.J. and Munson, C.A. (1996). Paleoliquefaction evidence for recurrent strong earthquakes since 20,000 years BP in the Wabash Valley of Indiana. *Final Report to the U.S. Geological Survey*, 137 p.

Munson, P.J., Obermeier, S.F., Munson, C.A., and Hajic, M.R. (1997). Liquefaction evidence for Holocene and latest Pleistocene seismicity in the southern halves of Indiana and Illinois – a preliminary overview. *Seismological Research Letters*, 68(4), 521-536.

Newman, E.J. (2007). Cone penetration testing in the interpretation of ground shaking from paleoliquefaction evidence. *PhD Thesis*, University of Illinois at Urbana-Champaign, Urbana, IL.

NRC (National Research Council). (1985). Liquefaction of soils during earthquakes. *Committee on Earthquake Engineering, Commission on Engineering and Technical Systems, National Research Council*, National Academy Press, Washington, DC, 240 p.

Obermeier, S.F. (1996). Use of liquefaction-induced features for paleoseismic analysis – an overview of how seismic liquefaction features can be distinguished from other features and how their regional distribution and properties can be used to infer the location and strength of Holocene paleo-earthquakes. *Engineering Geology*, 44, 1-76.

Obermeier, S.F. (1998a). Liquefaction evidence for strong earthquakes of Holocene and latest Pleistocene ages in the states of Indiana and Illinois, USA. *Engineering Geology*, 50, 227–254.

Obermeier, S.F. (1998b). Seismic liquefaction features: examples from paleoseismic investigations in the continental United States. *U.S. Geological Survey Open-File Report 98-488*.

Obermeier, S.F., Martin, J.R., Frankel, A.D, Youd, T.L., Munson, P.J., Munson, C.A., and Pond, E.C. (1993). Liquefaction evidence for one or more strong Holocene earthquakes in the Wabash Valley of southern Indiana and Illinois. *U.S. Geological Survey Professional Paper 1536*, 27 p.

Obermeier, S.F. and Pond, E.C. (1999). Issues in using liquefaction features for paleoseismic analysis. *Seismological Research Letters*, 70, 34-58.

Obermeier, S.F., Olson, S.M., and Green, R.A. (2005). Field occurrences of liquefaction-induced features: a primer for engineering geologic analysis of paleoseismic shaking. *Engineering Geology*, 76, 209-234.

Obermeier, S.F., Pond, E.C., and Olson, S.M., with contributions by Green, R.A., Mitchell, J.K., and Stark, T.D. (2001). Paleoliquefaction studies in continental settings – geologic and geotechnical factors in interpretations and back-analysis. *U.S. Geological Survey Open-File Report 01-029*, 75 p. <<http://pubs.usgs.gov/openfile/of01-029>>

Oda, M., Kawamoto, K., Suzuki, K., Fujimori, H., and Sato, M. (2001). Microstructural interpretation on reliquefaction of saturated granular soils under cyclic loading. *ASCE Journal of Geotechnical and Geoenvironmental Engineering*, 127(5), 416-423.

Olson, S.M., Green, R.A., and Obermeier, S.F. (2005a). Geotechnical analysis of paleoseismic shaking using liquefaction features: A major updating. *Engineering Geology*, 76, 235-261.

Olson, S.M., Green, R.A., and Obermeier, S.F. (2005b). Revised magnitude-bound relation for the Wabash Valley seismic zone of the central United States. *Seismological Research Letters*, 76(6), 756-771.

Olson, S.M., Muhammad, K., Wen, Y.K., and Song, J. (2007). Uncertainties in paleoliquefaction analysis: preliminary findings. *Proc., Geo-Denver*, Denver, CO.

- Olson, S.M., Obermeier, S.F., and Stark, T.D. (2001). Interpretation of penetration resistance for back-analysis at sites of previous liquefaction. *Seismological Research Letters*, 72(1), 46-59.
- Olson, S.M. and Stark, T.D. (1998). CPT based liquefaction resistance of sandy soils. *Proc., Specialty Conf. Geotechnical Earthquake Engineering and Soil Dynamics III*, ASCE, Aug. 3-6, Seattle, WA, Vol. 1, 325-336.
- Park, D. and Hashash, Y.M.A. (2005). Evaluation of seismic site factors in the Mississippi Embayment. II. Probabilistic seismic hazard analysis with nonlinear site effects. *Soil Dynamics and Earthquake Engineering*, 25, 145-156.
- Phoon, K.-K. and Kulhawy, F.H. (1999). Characterization of geotechnical variability. *Canadian Geotechnical Journal*, 36, 612-624.
- Pond, E.C. (1996). Seismic parameters for the central United States based on paleoliquefaction evidence in the Wabash Valley. *PhD Thesis*, Virginia Polytechnic Institute and State University, Blacksburg, VA, 583 p.
- Pond, E.C. and Martin, J.R. (1997). Estimated magnitudes and accelerations associated with prehistoric earthquakes in the Wabash Valley of the central United States. *Seismological Research Letters*, 68, 611-623.
- Power, M.S., Coppersmith, K.J., Youngs, R.R., Schwartz, D.P., and Swan, R.H. (1981). Seismic Exposure Analysis for the WNP-2 and WNP-1/4 Site: Appendix 2.5K to Amendment No. 18 Final Safety Analysis Report for WNP-2. Woodward-Clyde Consultants, San Francisco, 63 pp.
- Rhea, S. and Wheeler, R.L. (1996). Map showing seismicity in the vicinity of the lower Wabash Valley, Illinois, Indiana, and Kentucky. *U.S. Geological Survey Miscellaneous Investigation Map I-2583-A*, scale 1:250,000.
- Rodriguez-Marek, A., Bray, J.D., and Abrahamson, N.A. (2001). An empirical geotechnical seismic site response procedure. *Earthquake Spectra*, 17(1), 65-87.
- Schmertmann, J.H. (1991). The mechanical aging of soils. *ASCE Journal of Geotechnical Engineering*, 117, 1288-1330.
- Seed, H.B. and Idriss, I.M. (1971). Simplified procedure for evaluating liquefaction potential. *ASCE Journal of the Soil Mechanics and Foundations Division*, 97(9), 1249-1273.
- Seed, H.B., and Idriss, I.M. (1982). Ground motions and soil liquefaction during earthquakes. *Monograph Series*, Earthquake Engineering Research Institute, Oakland, CA, 134 p.
- Seed, H.B., Tokimatsu, K., Harder, L.F., and Chung, R.L. (1985). Influence of SPT procedures in soil liquefaction resistance evaluations. *ASCE Journal of Geotechnical Engineering*, 111(12), 1425-1445.

Seed, R.B. and Harder, L.F., Jr. (1990). SPT-based analysis of cyclic pore pressure generation and undrained residual strength. *Proc., H. Bolton Seed Memorial Symp.*, BiTech Publishers Ltd., Vancouver, 351-376.

Shibata, T., Oka, W., Ozawa, Y. (1996). Characteristics of ground deformation due to liquefaction. *Special Issue of Soils and Foundations on the Geotechnical Aspects of the January 17, 1995, Hyogoken-Nambu Earthquake*, 65-79.

Somerville, P., Collins, N., Abrahamson, N., Graves, R., and Saikia, C. (2001). Ground motion attenuation relations for the central and eastern United States. *Final Report to the U.S. Geological Survey*.

Somerville, P. and Moriwaki, Y. (2003). Seismic Hazards and Risk Assessment in Engineering Practice. *Chapter 65 in International Handbook of Earthquake and Engineering Seismology*, Volume 81B, W.H.K. Lee, H. Kanamori, P.C. Jennings, and C. Kisslinger, eds., 1945 pp.

Stewart, J.P., coordinator. (2001). Chapter 4: Soil liquefaction. Chi-Chi, Taiwan earthquake of September 21, 1999 reconnaissance report. J. Uzarski and C. Arnold, (eds.), *Earthquake Spectra*, Supplement A to Vol. 17, 37-60.

Stewart, J.P. (2003). Documentation of soil conditions at liquefaction sites from 1999 Chi-Chi, Taiwan earthquake. <[http://peer.berkeley.edu/lifelines/research\\_projects/3A02/](http://peer.berkeley.edu/lifelines/research_projects/3A02/)>

Street, R.L., Bauer, R.A., and Woolery, E.W. (2004). Short note: magnitude scaling of prehistorical earthquakes in the Wabash Valley seismic zone of the central United States, *Seismological Research Letters*, 75, 637-641.

Suzuki, Y., Tokimatsu, K., Moss, R.E.S., Seed, R.B., and Kayen, R.E. (2003). CPT-based liquefaction field case histories from the 1995 Hyogoken-Nambu (Kobe) earthquake, Japan. *Geotechnical Engineering Research Report No. UCB/GE-2003/03*, University of California at Berkeley, Berkeley, CA, 63 p.

Talwani, P. and Schaeffer, W.T. (2001). Recurrence rates of large earthquakes in the South Carolina Coastal Plain based on paleoliquefaction data. *Journal of Geophysical Research*, 106, 6621-6642.

Terzaghi, K., Peck, R.B., and Mesri, G. (1996). *Soil Mechanics in Engineering Practice, Third Edition*. John Wiley & Sons, Inc., New York, NY.

Tinsley, J.C. III, Egan, J.A., Kayen, R.E., Bennett, M.J., Kropp, A., and Holzer, T.L. (1998). Appendix: maps and descriptions of liquefaction and associated effects. *U.S. Geological Survey Professional Paper 1551-B*, U.S. Department of the Interior, 287-323.

Toprak, S., Holzer, T.L., Bennett, M.J., and Tinsley, J.C., III. (1999). CPT- and SPT-based probabilistic assessment of liquefaction potential. *Proc., 7<sup>th</sup> U.S.-Japan Workshop on Earthquake Resistant Design of Lifeline Facilities and Countermeasures Against Liquefaction*, Technical

Report MCEER-99-0019, Multidisciplinary Center for Earthquake Engineering Research, Buffalo, NY, 69-86.

Toro, G.R., Abrahamson, N.A., and Schneider, J.F. (1997). Model of strong ground motions from earthquakes in central and eastern North America: best estimates and uncertainties. *Seismological Research Letters*, 68(1), 41-57.

Tuttle, M., Cowie, P., Tinsley, J., Bennett, M.J., and Berrill, J. (1990a). Liquefaction and foundation failure of Chevron oil and gasoline tanks at Moss Landing, California. *Geophysical Research Letters*, 17(4), 56-74.

Tuttle, M. Law, K.T., Seeber, L., and Jacob, K. (1990b). Liquefaction and ground failure induced by the 1988 Saguenay, Quebec, earthquake. *Canadian Geotechnical Journal*, 27, 580-589.

Whitman, R.V. (1971). Resistance of soil to liquefaction and settlement. *Soils and Foundations*. 11(4), 59-68.

Youd, T.L. (1973). Ground movements in Van Norman Lake vicinity during San Fernando earthquake. In L.M. Murphy, ed., *San Fernando, California Earthquake of February 9, 1971*, vol. 3, U.S. Department of Commerce, U.S. Government Printing Office, Washington, DC, 197-206.

Youd, T.L. (1977). Brief review of liquefaction during earthquakes in Japan: discussion. *Soils and Foundations*, 17, 82-85.

Youd, T.L. and Bennett, M.J. (1983). Liquefaction sites, Imperial Valley, California. *ASCE Journal of Geotechnical Engineering*, 109(3), 440-457.

Youd, T.L., and Idriss, I.M. (eds.). (1997). Proceedings of the NCEER workshop on evaluation of liquefaction resistance of soils. *Technical Report NCEER-97-0022*, State University of New York at Buffalo, NY, 276 p.

Youd, T.L. and Noble, S.K. (1997). Liquefaction criteria based on statistical and probabilistic analysis. in T.L. Youd and I.M. Idriss, (eds.), *Proc. of the NCEER Workshop on Evaluation of Liquefaction Resistance of Soils*, Technical Report NCEER 97-0022, State University of New York at Buffalo, NY, 210-216.

Youd, T.L. and Wieczorek, G.F. (1982). Liquefaction and secondary ground failure. in *The Imperial Valley, California, Earthquake of October 15, 1979*, U.S. Geological Survey Prof. Paper 1254, U.S. Geological Survey, Menlo Park, CA, 223-246.

Youd, T.L., et al. (2001). Liquefaction resistance of soils: summary report from the 1996 NCEER and 1998 NCEER/NSF workshops on evaluation of liquefaction resistance of soils, *ASCE J. of Geotechnical and Geoenvironmental Engineering*, 127(4), 297-313.

Yuan, H., Yang, S.H., Andrus, R.D., and Juang, C.H. (2003). Liquefaction-induced ground failure: a study of the Chi-Chi earthquake cases. *Engineering Geology*, 17, 141-155.

## **PUBLICATIONS FROM THIS WORK**

Olson, S.M., Muhammad, K., Wen, Y.K., and Song, J. (2007). Uncertainties in paleoliquefaction analysis: preliminary findings. *Proc., Geo-Denver*, Denver, CO.

Olson, S.M., Song, J., Wen, Y.K., Johnson, C.I., and Muhammad, K. (2008). Quantifying uncertainties in paleoliquefaction back-analysis. Part I: treatment of uncertainties. *Engineering Geology*, in preparation.

Olson, S.M., Song, J., Wen, Y.K., Johnson, C.I., and Muhammad, K. (2008). Quantifying uncertainties in paleoliquefaction back-analysis. Part II: Vincennes earthquake example. *Engineering Geology*, in preparation.

Olson, S.M., Johnson, C.I., Song, J., and Wen, Y.K. (2008). Influence of liquefaction severity on liquefaction resistance relationships. *ASCE Journal of Geotechnical and Geoenvironmental Engineering*, in preparation.